Loss of SMAD3 promotes vascular remodeling in pulmonary arterial hypertension via MRTF disinhibition

Diana Zabini[1,2], Elise Granton[1], Yijie Hu[1], Maria Zena Miranda[1], Ulrike Weichelt[7], Sandra Breuils Bonnet[3], Sébastien Bonnet[3], Nicholas W Morrell[4], Kim A Connelly[1], Steeve Provencher[3], Bahil Ghanim[5], Walter Klepetko[5], Andrea Olschewski[2], Andras Kapus[1,6*], and Wolfgang M. Kuebler[1,6,7*].

[1]Keenan Research Centre for Biomedical Science, St. Michael´s Hospital, Toronto, Ontario, Canada; [2]Ludwig Boltzmann Institute for Lung Vascular Research, Graz, Austria, [3]Pulmonary Hypertension Group of the Institute of Cardiology and Pulmonology, Québec, Laval University, Quebec City, Canada, [4]Department of Medicine, University of Cambridge School of Clinical Medicine, Cambridge, UK, [5]Department of Thoracic Surgery, Medical University, Vienna, Austria [6]Dept. of Surgery, University of Toronto, Toronto, Ontario, Canada, and [7]Dept. of Physiology, Charité-Universitätsmedizin Berlin, Berlin, Germany.

*Corresponding Authors:

Andras Kapus, Email: KapusA@smh.ca, Tel: +1 416 847 1751; Address: Keenan Research Centre; 209 Victoria Street; Toronto; M5B 1T8; Canada

Wolfgang Kuebler, Email: wolfgang.kuebler@charite.de , Tel: +49 30 450 528501; Address: Charité-Universitätsmedizin Berlin, CharitéCrossOver (CCO) - Institute of Physiology; Virchowweg 6; 10117 Berlin; Germany

Author contributions: DZ, EG, SBB, YH, MZM, and UW conducted experiments. DZ, AK, and WMK designed experiments and analyzed the data. BG, WK, SB and NM provided human and murine cells and tissue samples. DZ, AK, and WMK drafted, and all authors edited the original manuscript.

Grant support: This work was supported by the Erwin-Schroedinger Fellowship of the Austrian FWF Foundation to DZ, and grants-in-aid from the Canadian Institutes of Health Research (CIHR) and the Heart & Stroke Foundation of Canada (HSFC) to WMK.

Running title: SMAD3 loss drives lung vascular remodeling in PH

Subject code: 3.12/ 3.15/9.2/17.6/17.10

Total word count: 3477

At a Glance Commentary:

Scientific Knowledge on the Subject: A considerable body of clinical and experimental data point towards a critical role for TGF-β signaling in the pathogenesis of pulmonary arterial hypertension; however, cellular mechanisms by which TGF-β promotes lung vascular remodeling remain unknown.

What This Study Adds to the Field: Loss of SMAD3 presents a novel pathomechanism in pulmonary arterial hypertension that promotes both proliferation and - via disinhibition of myocardin-related transcription factor - hypertrophy of pulmonary artery smooth muscle cells, thereby reconciling the parallel induction of a synthetic and contractile smooth muscle cell phenotype that promotes lung vascular remodeling in pulmonary hypertension.

"This article has an online data supplement, which is accessible from this issue's table of content online at www.atsjournals.org"

Abstract

Introduction: Vascular remodeling in pulmonary arterial hypertension (PAH) results from smooth muscle cell hypertrophy and proliferation of vascular cells. Loss of bone morphogenetic protein receptor 2 (BMPR-II) signaling and increased signaling via transforming growth factor β (TGF-β) and its downstream mediators SMAD2/3 has been proposed to drive lung vascular remodeling; yet, proteomic analyses indicate a loss of SMAD3 in PAH.

Objective: We proposed that SMAD3 may be dysregulated in PAH, and that loss of SMAD3 may present a pathophysiological master switch by disinhibiting its interaction partner myocardin-related transcription factor (MRTF) which drives muscle protein expression.

Methods and Results: SMAD3 was downregulated in lungs of PAH patients, and in pulmonary arteries of three independent PAH animal models. TGF-β treatment replicated the loss of SMAD3 in human pulmonary artery smooth muscle (huPASMCs) and endothelial (huPAECs) cells. *SMAD3* silencing increased proliferation and migration in huPASMCs and huPAECs. Co-immunoprecipitation revealed reduced interaction of MRTF with SMAD3 in TGF-β treated huPASMCs and pulmonary arteries of PAH animal models. In huPASMC, loss of SMAD3 or BMPR-II increased smooth muscle actin expression, which was attenuated by MRTF inhibition. Conversely, SMAD3 overexpression prevented TGF-β induced activation of a MRTF reporter and reduced actin stress fibers in *BMPR2* silenced huPASMC. MRTF inhibition attenuated PAH and lung vascular remodeling in sugen/hypoxia rats.

Conclusion: Loss of SMAD3 presents a novel pathomechanism in PAH that promotes vascular cell proliferation and - via MRTF disinhibition - hypertrophy of huPASMC, thereby reconciling the parallel induction of a synthetic *and* contractile huPASMC phenotype.

Introduction

Pulmonary arterial hypertension (PAH) is a rare but fatal disease, characterized by extensive remodeling of pulmonary arteries and muscularization of precapillary arterioles[1,2]. Clinical and experimental data point towards a central role for TGF-β signaling in PAH, in that a series of mutations in this pathway have been associated with PAH[3–10], and in that TGF-β expression is increased in pulmonary arteries and lungs of PAH patients and respective animal models[11,12].

By signaling through its canonical pathway, TGF-β, activates receptor-induced SMADs (R-SMADs, namely SMAD2 and SMAD3), which in turn promote gene expression involved in hypertrophy and fibrosis[13]. On a simplistic level, the documented elevated plasma levels for TGF-β in PAH[14,15] would therefore lead one to expect that SMADs downstream of TGF-β may play a crucial role in the pathogenesis of experimental or clinical PAH. Counterintuitively, however, a significant decrease in pulmonary SMAD3 expression was detected in PAH animal models as well as IPAH patients[11,12] in line with the fact that prolonged exposure to TGF-β can result in loss of SMAD3[16]. Hence, PAH may actually be associated with a decrease in the activity of the canonical TGF-β pathway.

While systemic cardiovascular diseases are commonly associated with a switch from a differentiated vascular smooth muscle cell phenotype with high expression of contractile proteins and low migration/proliferation abilities to a proliferative dedifferentiated phenotype with weak contractile protein expression and increased migration, proliferation and resistance to apoptosis[17–20], vascular remodeling in PAH is characterized by *both* dedifferentiation and increased smooth muscle cell (SMC) proliferation (hyperplasia), *as well as* an overall increase in smooth muscle protein (e.g. α-smooth muscle actin, SMA) expression characteristic of SMC hypertrophy[21]. As contractile and proliferative SMC phenotypes are

commonly considered mutually exclusive, the seeming contradiction of the parallel induction of both huPASMC hyperplasia *and* hypertrophy in PAH disease has so far remained enigmatic. Myocardin related transcription factor (MRTF) is a Rho GTPase responsive, actin-regulated transcriptional co-activator of serum response factor (SRF), a master regulator of muscle protein expression, including SMA that plays a crucial role in both maintenance of normal SMC homeostasis[22,23] and pathological vascular remodeling[24]. While the central role of MRTF in SMC hypertrophy renders it an attractive candidate contributor to vascular remodeling, MRTF dysregulation in PAH and its underlying mechanism has not yet been addressed.

MRTF dysregulation may be intrinsically linked to altered TGF-β signalling as suggested from our previous studies in kidney epithelial cells where we found SMAD3 capable of binding MRTF, thereby inhibiting MRTF-driven activation of the SMA promoter[25–28]**.** Since SMAD3 may concomitantly exert antiproliferative effects[29,30], a general loss of SMAD3 in PAH may drive both SMA expression via disinhibition of MRTF and huPASMC proliferation, and thus might explain the parallel existence of a hypertrophic *and* proliferative huPASMC phenotype in PAH[31–33]. To test this notion, we analysed SMAD3 expression levels in clinical samples and pre-clinical models of PAH, explored the protein-protein interaction between SMAD3 and MRTF, and their functional roles in huPASMC and pulmonary artery endothelial cells (huPAEC) relevant to the development and progression of PAH both *in vitro* and *in vivo.*

Methods

For full experimental details, including information on proliferation and migration assays, protein isolation and western blotting, RNA isolation and real-time PCR, cell transfection, co-immunoprecipitation, animal models of pulmonary hypertension and assessment of their endpoints please see the online supplement.

Human tissue samples. Human lung tissues were obtained from 7 controls who died unexpectedly from non-pulmonary causes and 7 PAH patients for which clinical characteristics are given in Supp. Table 1. Samples were collected under the ethic protocol #20773 at Laval University and used following current recommendations[34].

Cells. HuPASMC and huPAEC were purchased from Lonza, Promocell or isolated from downsized non-tumorous non-transplanted donor lungs (EK 976/2010, Medical University of Vienna) and cultured in Smooth Muscle or Endothelial Cell Growth Medium 2, respectively (Promocell). Murine PASMC were obtained from *BMPR2*$^{+/R899X}$ mice which carry a mutated allele of the *BMPR2* gene, and corresponding wild type mice as described[35].

Transfection. Pre-designed, commercially available siRNA sequences directed against human *SMAD3* and *BMPR2* were purchased (Dharmacon Thermo Sientific). For non-specific gene inhibition of the siRNAs used in this study, a universal negative-control siRNA sequence was used (Dharmacon Thermo Sientific). For SMAD3 overexpression a GFP-tagged Smad3 from Clonetech or a Myc-tagged Smad3 expression construct (in pCMV5B) was used. For MRTF overexpression a FLAG-tagged MRTF construct was used. Cells were transfected with 100nMol/L siRNA or 0.5-2µg plasmid for 8h.

Pulmonary hypertension models. The study was approved by the animal care and use committee of St. Michael´s, and experiments were performed in accordance with the "Guide for the Care and Use of Laboratory Animals" (Institute of Laboratory Animal Resources, 7th

edition 1996). For PAH induction in male Sprague-Dawley rats, both the sugen/hypoxia and the monocrotaline model were applied. Hemodynamic characterization was performed via right ventricular systolic pressure (RVSP) measurements and echocardiographic imaging of right ventricular function, and vascular remodelling and Fulton index were assessed *post mortem*.

Statistical analysis. All data are given as means±SEM. Student's t test (two-tailed) was used to compare two groups. Where appropriate, a two-way Analysis of Variance (ANOVA) was applied with Tukey´s post-hoc test. P-values < 0.05 were considered statistically significant.

Results

Smad3 is downregulated in clinical and preclinical PAH samples

Total SMAD3 protein levels were significantly decreased in lung lysates from 7 PAH patients as compared to healthy controls, while SMA expression was concomitantly elevated (Fig.1A-C). Reduced SMAD3 staining in the intima and media of pulmonary arteries was also evident by immunohistochemistry in IPAH patients as compared to donor lungs (Supp. Fig.1). Similar downregulation of SMAD3 was detected in pulmonary arteries of two animal models of PAH, the monocrotaline (MCT; Fig.1D,E) and the sugen/hypoxia rat model (Fig.1I,J), whereas TGF-β and smooth muscle actin expression were significantly upregulated in either model (Fig.1D,F,G,I,K,L). RVSP data for both PAH models are given in Fig.1H,M. To test whether chronic upregulation of TGF-β in PAH is sufficient to explain this loss in SMAD3, we probed for the effects of TGF-β on SMAD3 expression *in vitro*. While short-term exposure to TGF-β for 24h did not alter SMAD3 expression (data not shown), 72h treatment with 5 ng/mL TGF-β downregulated total SMAD3 levels in huPASMCs at both the protein and mRNA level (Fig.2A-C). Increasing TGF-β to 10ng/mL caused no further drop in SMAD3 levels, therefore all subsequent experiments were performed at 5 ng/mL. Decreased SMAD3 protein levels were similarly detectable in PAECs after 72h exposure to 5 or 10ng/mL TGF-β (Fig.2D,E). Likewise, hypoxia (1% O_2) as a trigger of pulmonary hypertension caused a significant drop in SMAD3 in huPASMCs at the protein (Fig.2F,G) and mRNA level (Fig.2H) as well as in PAECs (Fig.2I,J). Treatment with interleukin-6 or platelet-derived growth factor previously implicated in PAH pathogenesis did, however, not reduce SMAD3 expression in huPASMCs or huPAECs, suggesting that loss of SMAD3 expression is not a universal response to all PAH-related stimuli (Supp. Fig.2).

SMAD3 downregulation increases proliferation and migration

To test for functional consequences of SMAD3 loss, we silenced *SMAD3* in huPASMC by siRNA (Fig.3A,B) and assessed fetal calf serum (FCS)-induced proliferation in three independent assays. *SMAD3*-silenced huPASMCs exhibited i) higher protein levels for proliferating cell nuclear antigen (PCNA) (Fig.3A,C), ii) increased staining for nuclear Ki-67 (Fig.3D,E), and iii) higher bromodeoxyuridine (BrdU) levels (Fig.3F) as compared to control siRNA. A similar increase in FCS-induced proliferation was detectable as higher PCNA levels in *SMAD3*-silenced huPAECs relative to internal control (Fig.3G). Graph showing group data normalized towards siCTL is given in Supp. Figure 6B. Downregulation of SMAD3 also stimulated huPASMC (Fig. 3H) and huPAEC migration (Fig. 3I) towards an FCS gradient. Thus, downregulation of SMAD3 is sufficient to replicate two major features of PAH, enhanced proliferation and migration of huPASMC and huPAEC.

SMAD3 downregulation triggers smooth muscle cell hypertrophy

To test whether SMAD3 loss also triggers huPASMC hypertrophy, we assessed the effect of TGF-β treatment on the expression of SMA, a differentiation and hypertrophy marker in SMCs[36,37], and on the ratio of total protein to DNA content. TGF-β increased SMA expression and protein/DNA ratio in a time-dependent manner, which was associated with a concomitant decrease in SMAD3 levels (Fig.4A-C,E). In line with a direct link between SMAD3 loss and SMC hypertrophy, SMAD3 protein expression correlated inversely with both SMA expression (Fig.4D) and protein/DNA ratio (Fig.4F). Consolidating the notion that loss of SMAD3 directly contributes to increased SMA expression, we next showed that *SMAD3* silencing prior to TGF-β treatment augmented SMA expression in huPASMCs 24h after TGF-β (Fig.4G,H), whereas 72h after TGF-β no significant difference was observed between *SMAD3* silenced and control siRNA-transfected cells (Fig.4G,I). This observation is in accord with the fact that by 72h, TGF-β treatment *per se* caused a drop in SMAD3

(Fig.4A), thus minimizing the effect of additional SMAD3 silencing (Fig.4G). Taken together, these experiments substantiate that TGF-β-induced loss of SMAD3 promotes myogenic (hypertrophic) responses in SMC.

SMAD3-MRTF interaction is decreased by TGF-β treatment

In kidney tubular cells, we showed that SMAD3 interacts with MRTF[26] thereby inhibiting its effect on the SMA promoter[38]. To test for a similar scenario in PAH where TGF-β-dependent loss of SMAD3 may accordingly potentiate SMA expression via enhanced MRTF signaling, we probed for SMAD3-MRTF interaction by co-immunoprecipitation (co-IP). At baseline, MRTF pulled down substantial amounts of SMAD3, verifying the interaction of these proteins in resting huPASMCs. TGF-β treatment for 72h reduced the level of MRTF-associated SMAD3 (Fig.5A). This effect is likely attributable to the comparable reduction in total SMAD3 following TGF-β as evident in the co-IP input (Fig.5B) rather than a reduced affinity between the two proteins. Interaction between SMAD3 and MRTF was similarly reduced in pulmonary arteries of MCT (Fig.5C) or sugen-hypoxia (Fig.5D) treated rats, a finding that is in line with MRTF disinhibition in PAH.

To probe whether loss of SMAD3 may indeed prime cells for enhanced MRTF activity we treated huPASMC with sphingosine-1-phosphate (S1P), a trigger of MRTF nuclear translocation and activation[39,40]. In huPASMC treated with control siRNA, S1P induced SMA expression in an MRTF-dependent manner, as this effect was blocked by the MRTF inhibitor CCG1423 (Fig.6A). The latter effect was not attributable to induction of apoptosis by CCG1423, which could be effectively ruled out for both cell types (Supp.Fig.3&4). *SMAD3* silencing amplified S1P-induced SMA expression, which was again sensitive to MRTF inhibition consistent with an intensified MRTF-dependent signaling following SMAD3 loss (Fig.6A,B). Next, we expressed the MRTF/SRF-sensitive luciferase reporter 3DA in huPASMCs and showed that SMAD3 overexpression attenuated reporter activation in

response to either TGF-β stimulation (Fig.6E) or MRTF overexpression (Fig.6F), respectively, thus further validating the negative regulation of MRTF-dependent transcriptional activity by SMAD3. SMAD3 knock-down also enhanced FCS-induced proliferation in huPASMCs as assessed by BrdU assay, yet, this effect was not normalized by CCG1423 (Fig.6C). Similar results were obtained in huPAEC (Fig.6D), indicating that MRTF disinhibition contributes to hypertrophic yet not hyperplastic responses to loss of SMAD3 in lung vascular cells.

MRTF inhibition attenuates pulmonary hypertension and vascular remodelling in rats

Based on our findings that i) SMAD3 levels are decreased in clinical and preclinical PAH, and ii) that loss of SMAD3 drives MRTF-dependent SMA expression, we hypothesized that pharmacological inhibition of MRTF may alleviate vascular remodeling in experimental PAH. To address this question, PAH was induced by sugen/hypoxia, and rats were treated either in a prophylactic approach from day 0 or in a therapeutic approach from day 21 after SU5416 injection with daily injections of two different doses of CCG1423 or vehicle. As compared to untreated sugen/hypoxia animals, CCG1423-treated rats showed reduced lung vascular remodeling (Fig.7A,B) and RVSP (Fig.7C). Echocardiographic parameters of right ventricular (RV) function were, however, only normalized by prophylactic treatment with high dose CCG1423, but not with low dose prophylaxis or either therapeutic treatment dose (Fig.7D,E). This deviation of treatment effects on pulmonary hemodynamics and RV function may seem surprising; it is, however, in keeping with previous studies[41] which identified impaired RV function as a prominent feature of the sugen/hypoxia model that is not solely attributable to increased RV afterload, but involves additional direct or indirect effects on the RV that may be less responsive to MRTF inhibition.

Loss of functional BMPR-II causes SMAD3 loss which in turn drives PASMC hypertrophy

Loss of functional BMPR-II signaling, either due to inherited or spontaneous *BMPR2* gene mutations or to acquired loss of BMPR-II[42], is a key contributing factor in the pathogenesis of PAH[43,44]. To test for a link between impaired BMPR-II signaling and the SMAD3/MRTF-dependent regulation of huPASMC hypertrophy, we made use of a transgenic mouse model that overexpresses a mutated form of *BMPR2* (*BMPR2*$^{+/R899X}$) and gradually develops PAH[45]. In whole lung lysates of *BMPR2*$^{+/R899X}$ mice, total SMAD3 levels were markedly reduced as compared to controls (Fig.8A), indicating that loss of SMAD3 and subsequent MRTF disinhibition may contribute to lung vascular remodeling in cases of dysfunctional or deficient BMPR-II. In line with this view, PASMC isolated from *BMPR2*$^{+/R899X}$ mice had increased SMA and PCNA expression (Fig.8B,C) as well as decreased total SMAD3 and BMPR-II protein levels.

To assess if impaired BMPR-II signaling may *per se* account for loss of SMAD3, we silenced *BMPR2* in huPASMCs which markedly decreased SMAD3 expression (Fig.9A-C). Consistent with the concept of MRTF disinhibition, SMA expression in response to S1P was enhanced in *BMPR2* silenced cells, and this effect was prevented by CCG1423 (Fig.9A,D). Silencing of *BMPR2* also increased TGF-β expression in huPASMC, providing for a potential mechanistic link between BMPR-II and TGF-β (Fig.9E-G). Interestingly, MRTF inhibition also reduced the expression of both SMAD3 and BMPR-II in siCTL-treated cells, a finding that not only corroborates the tight link of SMAD3 expression to the abundance of functional BMPR-II, but also suggests that BMPR-II expression may be negatively regulated by MRTF in a homeostatic feedback loop. To link elevated SMA expression in response to S1P in *BMPR2* silenced cells directly to the loss of SMAD3, we additionally transfected huPASMC with a SMAD3 expressing plasmid to test whether reconstitution of SMAD3 may reverse the increase in SMA expression in S1P stimulated, *BMPR2* silenced cells. The latter notion was confirmed, in that *BMPR2* silencing increased the formation of actin stress fibers

and phalloidin staining in S1P-stimulated huPASMC, yet this effect was antagonized and baseline phalloidin staining reduced in huPASMC overexpressing SMAD3 (Fig.10).

Discussion

In the present study we identified loss of SMAD3 as characteristic hallmark in different PAH-related scenarios, and as central pathophysiological mechanism in lung vascular remodeling. Loss of SMAD3 drives PASMC hypertrophy via disinhibition of MRTF, while concomitantly stimulating PASMC and PAEC proliferation in an MRTF-independent manner. Importantly, these findings not only identify a novel shared and potentially targetable signaling pathway of vascular remodeling in PAH, but also reconcile the seemingly contradictory parallel stimulation of both contractile and synthetic PASMC phenotypes in PAH. Induction of this pathway by BMPR-II dysfunction or deficiency provides for a novel explanation for the propensity of patients with spontaneous or inherited *BMPR2* mutations to develop PAH, and – as we discuss later - resolves the conceptual dilemma how functional BMPR-II deficiency may promote vascular remodeling given that BMP/BMPR-II signaling *per se* induces PASMC differentiation.

In line with previous reports indicating that SMAD3 may be downregulated in experimental PAH[11], we demonstrate here loss of SMAD3 in i) human lung samples of PAH patients, ii) pulmonary arteries from two preclinical models of PAH, iii) cultured huPASMC stimulated by TGF-β or hypoxia, iv) a mouse model bearing a heterozygous knock-in allele of a human *BMPR2* mutation, or v) *BMPR2*-silenced huPASMC. As such, loss of SMAD3 emerges as a common hallmark in different scale models of PAH disease. The mechanism of SMAD3 downregulation in PAH was not focus of the present work, but is potentially attributable to

epigenetic regulation via miR-199a-5p, which is upregulated in rat models of PH[46] and negatively regulates SMAD3 expression in huPAEC and huPASMC[46].

The role of SMAD3 in cell signaling has classically been viewed primarily in terms of its function as transcriptional modulator that, upon stimulation of the TGF-β type I receptor, becomes phosphorylated and, together with SMAD4, translocates to the nucleus where it regulates the transcription of various TGF-β target genes by binding to the SBE (SMAD-binding element) in their promoter region[47]. Here, we describe a fundamentally different role of SMAD3 in the regulation of TGF-β induced gene expression, which is independent of its phosphorylation and nuclear translocation, but relates to its overall downregulation in response to TGF-β or in pulmonary hypertension[25,48,49]. In huPASMC and huPAEC, silencing of *SMAD3* replicated key mechanisms of lung vascular remodeling in PAH, namely cell proliferation, migration, and – in case of huPASMC – hypertrophy. The parallel induction of both hyperplastic and hypertrophic responses by SMAD3 loss reconciles these seemingly opposing effects in a single molecule.

Induction of hypertrophy was attributable to a liberation of the myogenic transcription factor MRTF from a tonic SMAD3-mediated inhibition. The relevance of SMAD3-MRTF interaction in vascular homeostasis, and the role of MRTF disinhibition following SMAD3 loss was documented in a series of experiments, in that SMAD3 was shown to co-immunoprecipitate with MRTF in huPASMC at rest, yet MRTF was released from this interaction upon TGF-β treatment due to loss of SMAD3. Notably, our co-immunoprecipitation experiments focused on MRTF-B; however, we have previously documented a similar disinhibition by SMAD3 loss for MRTF-A in kidney epithelial cells[50], suggesting a potential synergistic role of both MRTFs in PAH. A similar reduction in SMAD3-MRTF interaction was detected in pulmonary arteries from sugen/hypoxia or MCT treated rats. MRTF disinhibition then promotes cell hypertrophy, as demonstrated by the

finding that *SMAD3* silencing amplified SMA expression in response to S1P in an MRTF-inhibitor sensitive manner. Conversely, SMAD3 overexpression attenuated the activation of a MRTF/SRF reporter in response to TGF-β or MRTF overexpression. The relevance of this signaling pathway in the context of PAH was confirmed in the sugen/hypoxia model, in that both prophylactic and therapeutic treatment of rats with an MRTF inhibitor attenuated lung vascular remodeling and hemodynamic changes. In contrast, MRTF disinhibition did not contribute to the proliferative effect of SMAD3 loss, since proliferation in response to *SMAD3* silencing was not attenuated by MRTF inhibition.

BMPR2 presents the single most prominent gene implicated in PAH, in that missense, frame-shift, or nonsense mutations in *BMPR2* are present in 70% of families with familial PAH, and in up to 25% of patients with sporadic idiopathic PAH[14]. Loss of functional BMPR-II signaling extends, however, beyond *BMPR2* mutations, as acquired loss of BMPR-II is a common trait in nongenetic forms of PAH in humans[42] and animal models[51]. The mechanism by which functionally relevant mutations or acquired loss of BMPR-II promote PAH has traditionally been attributed to a shift from a BMPR-II-dependent, SMAD1/5/8 mediated homeostatic vascular phenotype to a TGF-β-driven, SMAD2/3-mediated vascular remodeling[14]. In the present study, however, we show that SMAD3 is largely lost in PASMC carrying the *BMPR2* mutation R899X, or following *BMPR2* silencing, while loss of *BMPR2* increased TGF-β expression. This finding is reconcilable with an initial predominance of TGF-β/SMAD2/3 signaling in *BMPR2* mutated or silenced cells, which in turn, however, results in a loss of SMAD3 (Fig. 11). Hence, rather than promoting a long-term increase in SMAD2/3 signaling, functional loss of BMPR-II may promote PASMC hypertrophy via disinhibition of MRTF due to loss of SMAD3. Two findings confirm this notion: First, *BMPR2* silencing increased S1P-induced SMA expression in huPASMC in an MRTF-dependent manner. Second, overexpression of SMAD3 prevented the formation of actin

stress fibers in huPASMC in response to *BMPR2* silencing. While these findings establish loss of SMAD3 and subsequent MRTF disinhibition as important mechanisms driving PASMC hypertrophy following functional loss of BMPR-II signaling, the role of MRTF in BMPR-II signaling and lung vascular homeostasis is slightly more complex: Activation of BMPR-II by BMPs stimulates itself MRTF via the RhoA/ROCK pathway[22,23], an effect that has been proposed to maintain the non-proliferative, differentiated PASMC phenotype in the healthy pulmonary vasculature[22]. Conversely, we demonstrate here an important role for MRTF signaling in PASMC hypertrophy and PAH development. Thus, MRTF's regulation differs under healthy (BMPR-dominated) and pathological (TGF-β dominated) conditions. In the former case MRTF is temporarily activated by BMPR-II and contributes to the maintenance of the contractile phenotype. In the latter case, MRTF acts on the background of SMAD3 loss, i.e. in the absence of its tonic inhibitor. This results in prolonged (dysregulated) MRTF activation, provoking a hypertrophic response that coincides with hyper-proliferation as an independent consequence of SMAD3 loss. Thus, instead of the normal time-segregation between proliferative or synthetic responses, PAH is characterized by parallel existence of both.

The recognition of SMAD3 expression levels as important master switch in the pathogenesis of PAH not only identifies loss of SMAD3 as new cellular pathomechanism of lung vascular remodelling, but also constitutes in our view an important conceptual advance in that the concurrent stimulation of proliferative and hypertrophic signaling pathways reconciles the seemingly mutually exclusive, parallel induction of a synthetic *and* contractile huPASMC phenotype, and recognizes MRTF signaling as a double-edged sword that maintains BMP-regulated vascular homeostasis in the healthy lung, while similarly driving TGF-β induced lung vascular remodeling in PAH.

368 Disclosures: Authors have nothing to disclose

369

370

References

1. Stenmark, K., Fagan, K. & Frid, M. Hypoxia-Induced Pulmonary Vascular Remodeling: Cellular and Molecular Mechanisms. *Circ. Res.* (2006).
2. Humbert, M. *et al.* Cellular and molecular pathobiology of pulmonary arterial hypertension. in *Journal of the American College of Cardiology* **43,** (2004).
3. Trembath, R. C. *et al.* Clinical and molecular genetic features of pulmonary hypertension in patients with hereditary hemorrhagic telangiectasia. *N. Engl. J. Med.* **345,** 325–334 (2001).
4. Newman, J. H. *et al.* Mutation in the gene for bone morphogenetic protein receptor II as a cause of primary pulmonary hypertension in a large kindred. *N. Engl. J. Med.* **345,** 319–324 (2001).
5. Lane, K. B. *et al.* Heterozygous germline mutations in BMPR2, encoding a TGF-beta receptor, cause familial primary pulmonary hypertension. *Nat. Genet.* **26,** 81–84 (2000).
6. Deng, Z. *et al.* Familial primary pulmonary hypertension (gene PPH1) is caused by mutations in the bone morphogenetic protein receptor-II gene. *Am. J. Hum. Genet.* **67,** 737–744 (2000).
7. Chaouat, A. *et al. Endoglin germline mutation in a patient with hereditary haemorrhagic telangiectasia and dexfenfluramine associated pulmonary arterial hypertension. Thorax* **59,** 446–448 (2004).
8. Harrison, R. E. *et al.* Molecular and functional analysis identifies ALK-1 as the predominant cause of pulmonary hypertension related to hereditary haemorrhagic telangiectasia. *J. Med. Genet.* **40,** 865–871 (2003).
9. Yeager, M. E., Halley, G. R., Golpon, H. A., Voelkel, N. F. & Tuder, R. M. Microsatellite instability of endothelial cell growth and apoptosis genes within

plexiform lesions in primary pulmonary hypertension. *Circ. Res.* **88,** E2–E11 (2001).

10. Massagué, J., Blain, S. W. & Lo, R. S. TGFbeta signaling in growth control, cancer, and heritable disorders. *Cell* **103,** 295–309 (2000).

11. Zakrzewicz, a *et al.* The transforming growth factor-beta/Smad2,3 signalling axis is impaired in experimental pulmonary hypertension. *Eur. Respir. J.* **29,** 1094–104 (2007).

12. Richter, A. *et al.* Impaired transforming growth factor-beta signaling in idiopathic pulmonary arterial hypertension. *Am. J. Respir. Crit. Care Med.* **170,** 1340–1348 (2004).

13. Broide, D. H. Immunologic and inflammatory mechanisms that drive asthma progression to remodeling. *J. Allergy Clin. Immunol.* **121,** 560–70; quiz 571–2 (2008).

14. Morrell, N. W. Pulmonary hypertension due to BMPR2 mutation: a new paradigm for tissue remodeling? *Proc. Am. Thorac. Soc.* **3,** 680–6 (2006).

15. Harrison, R. *et al.* Transforming growth factor-beta receptor mutations and pulmonary arterial hypertension in childhood. (2005).

16. Yanagisawa, K. *et al.* Induction of apoptosis by Smad3 and down-regulation of Smad3 expression in response to TGF-beta in human normal lung epithelial cells. *Oncogene* **17,** 1743–1747 (1998).

17. Watanabe, N. *et al.* BTEB2, a Kruppel-Like Transcription Factor, Regulates Expression of the SMemb/Nonmuscle Myosin Heavy Chain B (SMemb/NMHC-B) Gene. *Circ. Res.* **85,** 182–191 (1999).

18. Owens, G. K., Kumar, M. S. & Wamhoff, B. R. Molecular regulation of vascular smooth muscle cell differentiation in development and disease. *Physiol. Rev.* **84,** 767–801 (2004).

19. Nishimura, G. *et al.* DeltaEF1 mediates TGF-beta signaling in vascular smooth muscle

cell differentiation. *Dev Cell* **11,** 93–104 (2006).

20. Vaillancourt, M., Ruffenach, G., Meloche, J. & Bonnet, S. Adaptation and remodelling of the pulmonary circulation in pulmonary hypertension. *Canadian Journal of Cardiology* **31,** 407–415 (2015).

21. Deng, H. *et al.* Pulmonary artery smooth muscle hypertrophy: roles of glycogen synthase kinase-3beta and p70 ribosomal S6 kinase. *Am J Physiol Lung Cell Mol Physiol* **298,** L793–803 (2010).

22. Lagna, G. *et al.* Control of phenotypic plasticity of smooth muscle cells by bone morphogenetic protein signaling through the myocardin-related transcription factors. *J. Biol. Chem.* **282,** 37244–55 (2007).

23. Wang, D. *et al.* Bone morphogenetic protein signaling in vascular disease: anti-inflammatory action through myocardin-related transcription factor A. *J. Biol. Chem.* **287,** 28067–77 (2012).

24. Minami, T. *et al.* Reciprocal expression of MRTF-A and myocardin is crucial for pathological vascular remodelling in mice. *The EMBO Journal* (2012).

25. Masszi, A. & Kapus, A. Smaddening complexity: the role of Smad3 in epithelial-myofibroblast transition. *Cells. Tissues. Organs* **193,** 41–52 (2011).

26. Masszi, A. *et al.* Fate-determining mechanisms in epithelial-myofibroblast transition: major inhibitory role for Smad3. *J. Cell Biol.* **188,** 383–99 (2010).

27. Charbonney, E., Speight, P., Masszi, A., Nakano, H. & Kapus, A. β-catenin and Smad3 regulate the activity and stability of myocardin-related transcription factor during epithelial-myofibroblast transition. *Mol. Biol. Cell* **22,** 4472–85 (2011).

28. Speight, P., Kofler, M., Szászi, K. & Kapus, A. Context-dependent switch in chemo/mechanotransduction via multilevel crosstalk among cytoskeleton-regulated MRTF and TAZ and TGFβ-regulated Smad3. *Nat. Commun.* **7,** 11642 (2016).

29. Reisdorf, P., Lawrence, D. a, Sivan, V., Klising, E. & Martin, M. T. Alteration of transforming growth factor-beta1 response involves down-regulation of Smad3 signaling in myofibroblasts from skin fibrosis. *Am. J. Pathol.* **159,** 263–272 (2001).

30. Brown, K. A., Pietenpol, J. A. & Moses, H. L. A tale of two proteins: Differential roles and regulation of Smad2 and Smad3 in TGF-?? signaling. *Journal of Cellular Biochemistry* **101,** 9–33 (2007).

31. Nicolás, F. J., Lehmann, K., Warne, P. H., Hill, C. S. & Downward, J. Epithelial to mesenchymal transition in madin-darby canine kidney cells is accompanied by down-regulation of Smad3 expression, leading to resistance to transforming growth factor-β-induced growth arrest. *J. Biol. Chem.* **278,** 3251–3256 (2003).

32. Daly, A. C., Vizán, P. & Hill, C. S. Smad3 protein levels are modulated by ras activity and during the cell cycle to dictate transforming growth factor-β responses. *J. Biol. Chem.* **285,** 6489–6497 (2010).

33. Onwuegbusi, B. A., Rees, J. R. E., Lao-Sirieix, P. & Fitzgerald, R. C. Selective loss of TGFβ Smad-dependent signalling prevents cell cycle arrest and promotes invasion in oesophageal adenocarcinoma cell lines. *PLoS One* **2,** (2007).

34. Bonnet, S. *et al.* Translating Research into Improved Patient Care in Pulmonary Arterial Hypertension. *Am. J. Respir. Crit. Care Med.* 1–39 (2016). doi:10.1164/rccm.201607-1515PP

35. Han, C. *et al.* SMAD1 deficiency in either endothelial or smooth muscle cells can predispose mice to pulmonary hypertension. *Hypertension* **61,** 1044–52 (2013).

36. Stephenson, L. A., Haney, L. B., Hussaini, I. M., Karns, L. R. & Glass, W. F. Regulation of smooth muscle ??-actin expression and hypertrophy in cultured mesangial cells. *Kidney Int.* **54,** 1175–1187 (1998).

37. Masszi, A. *et al.* Central role for Rho in TGF-beta1-induced alpha-smooth muscle

actin expression during epithelial-mesenchymal transition. *Am. J. Physiol. Renal Physiol.* **284,** F911–F924 (2003).

38. Masszi, A. & Kapus, A. Smaddening complexity: The role of Smad3 in epithelial-myofibroblast transition. *Cells Tissues Organs* **193,** 41–52 (2010).

39. Lockman, K. *et al.* Sphingosine 1-phosphate stimulates smooth muscle cell differentiation and proliferation by activating separate serum response factor co-factors. *J. Biol. Chem.* **279,** 42422–30 (2004).

40. Castaldi, A. *et al.* Sphingosine 1-phosphate elicits RhoA-dependent proliferation and MRTF-A mediated gene induction in CPCs. *Cell. Signal.* **28,** 871–879 (2016).

41. Bogaard, H. J. *et al.* Chronic pulmonary artery pressure elevation is insufficient to explain right heart failure. *Circulation* **120,** 1951–1960 (2009).

42. Atkinson, C. Primary Pulmonary Hypertension Is Associated With Reduced Pulmonary Vascular Expression of Type II Bone Morphogenetic Protein Receptor. *Circulation* **105,** 1672–1678 (2002).

43. Sawada, H. *et al.* Reduced BMPR2 expression induces GM-CSF translation and macrophage recruitment in humans and mice to exacerbate pulmonary hypertension. *J. Exp. Med.* **211,** 263–80 (2014).

44. Hopper, R. K. *et al.* In Pulmonary Arterial Hypertension, Reduced BMPR2 Promotes Endothelial-to-Mesenchymal Transition via HMGA1 and its Target Slug. *Circulation* (2016). doi:10.1161/CIRCULATIONAHA.115.020617

45. Long, L. *et al.* Selective enhancement of endothelial BMPR-II with BMP9 reverses pulmonary arterial hypertension. *Nat. Med.* **21,** 777–85 (2015).

46. Liu, Y., Liu, G., Zhang, H. & Wang, J. MiRNA-199a-5p influences pulmonary artery hypertension via downregulating Smad3. *Biochem. Biophys. Res. Commun.* **473,** 859–866 (2016).

47. Wang, G., Matsuura, I., He, D. & Liu, F. Transforming growth factor-{beta}-inducible phosphorylation of Smad3. *J. Biol. Chem.* **284,** 9663–73 (2009).

48. Zhao, Y. & Geverd, D. A. Regulation of Smad3 expression in bleomycin-induced pulmonary fibrosis: a negative feedback loop of TGF-beta signaling. *Biochem. Biophys. Res. Commun.* **294,** 319–23 (2002).

49. Poncelet, A. C., Schnaper, H. W., Tan, R., Liu, Y. & Runyan, C. E. Cell phenotype-specific down-regulation of Smad3 involves decreased gene activation as well as protein degradation. *J. Biol. Chem.* **282,** 15534–15540 (2007).

50. Masszi, A. *et al.* Fate-determining mechanisms in epithelial-myofibroblast transition: Major inhibitory role for Smad3. *J. Cell Biol.* **188,** 383–399 (2010).

51. Long, L. *et al.* Altered bone morphogenetic protein and transforming growth factor-?? signaling in rat models of pulmonary hypertension. Potential for activin receptor-like kinase-5 inhibition in prevention and progression of disease. *Circulation* **119,** 566–576 (2009).

Figure legends

Figure 1: SMAD3 protein expression is decreased and SMA and TGF-β protein expression is increased in clinical samples and preclinical models of pulmonary arterial hypertension (PAH). Representative western blots (A,D,I) and corresponding densitometric quantification (B,C,E-G, J-L) show SMAD3 and SMA expression in (A-C) total lung lysates of 7 PAH patients as compared to healthy sex- and age-matched controls (CTL; n=7), and SMAD3, SMA and TGF-β expression in rat pulmonary arteries after (D-G) 3 weeks of monocrotaline (MCT) treatment relative to untreated controls (n=8 each), or (I-L) after Sugen/hypoxia (Su/hyp) relative to untreated controls (n=4 each). RVSP values for MCT and Su/hyp rats used for protein expression analyses are shown (H,M).*P<0.05 vs. CTL. T-test was applied.

Figure 2: Stimulation with transforming growth factor-β or hypoxia decreases SMAD3 expression in pulmonary vascular cells. **A-E:** Representative western blots (A,D), corresponding densitometric quantification (B,E; n=4-5 independent experiments each) and mRNA expression levels as determined by real-time PCR (C) show SMAD3 expression in human pulmonary artery smooth muscle cells (huPASMC; A-C) and human pulmonary artery endothelial cells (huPAEC; D,E) after 72h stimulation with either 5 or 10 ng/mL transforming growth factor (TGF)-β, or vehicle control (CTL), respectively. *P<0.05 vs. CTL. **F-J:** Representative western blots (F,I), corresponding densitometric quantification (G,J; n=2-3 independent experiments each) and mRNA expression levels as determined by real-time PCR (H) show SMAD3 expression in huPASMC (F-H) and huPAEC (I,J) after 72h stimulation with either 5 ng/mL TGF-β or vehicle control (CTL) in normoxia (21% O_2) or hypoxia (1 %O_2), respectively. *P<0.05 vs. CTL; Two-way ANOVA was applied with Tukey´s post-hoc test.

Figure 3: SMAD3 downregulation increases proliferation and migration in pulmonary vascular cells. **A-C:** Representative western blots (A) and corresponding densitometric quantification of SMAD3 (B) and proliferating cell nuclear antigen (PCNA; C) levels (n=4 independent experiments each) show increased PCNA levels upon stimulation with fetal calf serum (FCS; 5% for 24h) in human pulmonary artery smooth muscle cells (huPASMC) treated with SMAD3-specific (siSMAD3) relative to control (siCTL) siRNA. **P*<0.05 vs. CTL; #*P*<0.05 vs. siSMAD3+FCS. **D-F:** Representative fluorescence microscopic images of huPASMC immmunostained for Ki-67 (red; marked by arrows) and counterstained with 4',6-diamidino-2-phenylindole (DAPI; blue) (D), corresponding quantification of proliferating (Ki-67$^+$) cells per image field (E) and quantitative measurement of bromodeoxyuridine (BrdU) incorporation into huPASMC (F) show increased FCS-induced proliferation in siSMAD3-treated relative to siCTL-treated huPASMC (n=3-4 independent experiments each). **P*<0.05 vs CTL; #*P*<0.05 vs. siCTL+FCS. **G:** Densitometric quantification (n=3-4 independent experiments each) shows increased PCNA levels upon FCS stimulation in siSMAD3-treated relative to siCTL-treated human pulmonary artery endothelial cells (huPAEC; n=3-4 independent experiments each). **P*<0.05 vs. CTL; #*P*<0.05 vs. siCTL+FCS. **H,I:** Bar graphs show migration of siSMAD3-treated or siCTL-treated huPASMC (H) or huPAEC (I) in response to FCS stimulation (n>3 independent experiments each). **P*<0.05 vs. CTL; *P*#<0.05 vs. siSMAD3+FCS, *P*§<0.05 vs. siCTL+FCS. Two-way ANOVA was applied with Tukey´s post-hoc test.

Figure 4: SMAD3 downregulation triggers smooth muscle cell hypertrophy. **A-C**: Representative western blots (A) and corresponding densitometric quantification of smooth muscle actin (SMA; B) and SMAD3 (C) levels (n=4-5 independent experiments each) show time-dependent increase in SMA expression and parallel loss of SMAD3 in human

pulmonary artery smooth muscle cells (huPASMC) treated with transforming growth factor (TGF)-β (5 ng/mL). *P<0.05 vs. CTL. **D**: Expression levels of SMA and SMAD3 at identical time points post TGF-β treatment follow a near-linear inverse relationship as determined by linear regression analysis (dotted line). **E:** Group data show protein/DNA ratios in huPASMC at different time points post TGF-β treatment. **F:** Protein/DNA ratios and SMAD3 protein expression levels at identical time points post TGF-β treatment follow an inverse relationship. **G-I:** Representative western blots (**G**) and corresponding densitometric quantification (n=4-5 independent experiments each) show increased SMA expression in huPASMC treated with SMAD3-specific (siSMAD3) relative to control (siCTL) siRNA at 24h of TGF-β treatment (**H**; lanes with dotted circumference in **G**), yet not at 72h (**I**; lanes with continuous circumference in **G**). *P<0.05 vs. CTL(B, C; E) or siCTL (H);respectively, n.s., not significant. Two-way ANOVA was applied with Tukey´s post-hoc test.

Figure 5: SMAD3-MRTF interaction is decreased by transforming growth factor-β treatment. **A,B:** Human pulmonary artery smooth muscle cells (huPASMC) were treated for 72h with transforming growth factor (TGF)-β (5 ng/mL) or vehicle (CTL), immunoprecipitated (IP) with a myocardin-related transcription factor (MRTF) antibody, and precipitated pellets and supernatant (SUP; showing effective MRTF depletion by IP) were immunoblotted (IB) for MRTF-B and SMAD3 (A). Densitometric quantification reveals reduced co-immunoprecipitation (Co-IP) of SMAD3 with MRTF that is quantitatively comparable to the reduction in total SMAD3 by TGF-β in the input used for the IP (B, n=4 independent experiments). **C,D:** Pulmonary arteries isolated from monocrotaline- (MCT; C; full blot see Supp. Figure 6A) or Sugen-hypoxia (Su/hyp) treated rats and corresponding controls (CTL; n=4-5 independent experiments each) were immunoprecipitated with an MRTF-antibody, and immunoblotted for MRTF and SMAD3. Densitometric quantification

586 demonstrates reduced Co-IP of SMAD3 with MRTF in experimental models of pulmonary
587 arterial hypertension. *P<0.05 vs. CTL.T-test was applied.
588
589 **Figure 6:** Loss of SMAD3 primes for enhanced MRTF activity. **A,B:** Representative western
590 blots of smooth muscle actin (SMA) and SMAD3 (A) and corresponding densitometric
591 quantification of SMA (B) levels (n=5 independent experiments each) show increased
592 expression of SMA following myocardin-related transcription factor (MRTF) activation by
593 sphingosine-1-phosphate (S1P; 1 µMol/L) in human pulmonary artery smooth muscle cells
594 (huPASMC) treated with SMAD3-specific (siSMAD3) relative to control (siCTL) siRNA
595 that is sensitive to MRTF inhibition by CCG1423 (5µMol/L). *P<0.05 vs. siCTL+S1P;
596 #P<0.05 vs. siSMAD3+S1P. **C-D:** Quantitative measurement of bromodeoxyuridine (BrdU)
597 incorporation into huPASMC (C) or huPAEC (D) shows increased proliferation in response
598 to fetal calf serum (FCS; 5%) as compared to vehicle in both siCTL- and siSMAD3-treated
599 huPASMC or huPAEC, and increased BrdU incorporation in siSMAD3 as compared to
600 siCTL-treated, FCS-stimulated huPASMC or huPAECs that is, however, not reversed by the
601 MRTF inhibitor CCG1423 (n>3 independent experiments each). *P<0.05 vs. siCTL;
602 #P<0.05 vs. siCTL+ CCG1423; §P<0.05 vs. siSMAD3; $$P$<0.05 vs. siSMAD3+CCG1423.
603 Two-way ANOVA was applied with Tukey´s post-hoc test. **E-F:** Group data show luciferase
604 reporter activity of the MRTF/SRF sensitive promoter 3DA in TGF-β treated huPASMCs
605 overexpressing an empty-GFP or SMAD3-GFP plasmid (**E**; n=3 each) or huPASMCs co-
606 expressing MRTF-FLAG with an empty-GFP or SMAD3-GFP overexpressing plasmid (F,
607 n=3). *P<0.05 vs. CTL. T-test was applied.
608
609

Figure 7: MRTF inhibition attenuates pulmonary hypertension and vascular remodelling in rats. Representative hematoxylin & eosin stainings show lung vascular remodelling (**A**), and bar graphs show vascular wall thickness relative to vessel diameter in lung microvessels of <50 µm, 50-100 µm, and >100 µm diameter (**B**), right ventricular systolic pressure (RVSP; **C**), and echocardiographic analysis of tricuspid anular plane systolic excursion (TAPSE; **D**) and pulmonary artery acceleration time (PAAT; **E**). Rats were either kept under normoxic conditions, or underwent treatment with Sugen/hypoxia (Su/hyp) for induction of pulmonary arterial hypertension, and were treated with either vehicle (DMSO), the myocardin-related transcription factor (MRTF) inhibitor CCG1423 (0.15mg/kg), or a five-fold higher dose of CCG1423 (0.75mg/kg; 5xCCG1423) from day 0 or as therapeutic approach from day 21 after SU5416 injection (n=5-10 rats per group). **P*<0.05 vs normoxic vehicle control, #*P*<0.05 vs Su/hyp+vehicle.

Figure 8: Loss of functional bone morphogenetic protein receptor 2 causes downregulation of SMAD3. **A:** Representative western blots show SMAD3 protein expression in total lung lysates of *BMPR2*$^{+/R899X}$ and corresponding wild type (WT) mice (replicated in n=3 independent experiments each). **B,C:** Representative western blots and corresponding densitometric quantification of bone morphogenetic protein receptor 2 (BMPR-II), smooth muscle actin (SMA), proliferating cell nuclear antigen (PCNA), and SMAD3 show loss of BMPR-II and SMAD3, and increased proliferation and SMA expression in pulmonary artery smooth muscle cells isolated from lungs of *BMPR2*$^{+/R899X}$ mice as compared to those from WT mice (n=4 independent experiments each). **P*<0.05 vs. WT. T-test was applied.

Figure 9: Loss of functional bone morphogenetic protein receptor 2 drives smooth muscle hypertrophy in a myocardin-related transcription factor and SMAD3 dependent manner. **A-**

C: Representative western blots (A) and corresponding densitometric quantification show (B) successful *BMPR2* silencing, (C) loss of SMAD3 in human pulmonary artery smooth muscle cells (huPASMC) treated with *BMPR2*-specific (siBMPR2) relative to control (siCTL) siRNA, and (D) increased expression of smooth muscle actin (SMA) following myocardin-related transcription factor (MRTF) activation by sphingosine-1-phosphate (S1P; 1 µMol/L) in siBMPR2-treated as compared to siCTL-treated huPASMC that is sensitive to MRTF inhibition by CCG1423 (5 µMol/L) (n=9 independent experiments each). **P*<0.05 vs siCTL; #*P*<0.05 vs siBMPR2+S1P. T-Test was applied. **E-G:** Representative western blots (E) and corresponding densitometric quantification show increased TGF-β (F) expression after *BMPR2* silencing (G).

Figure 10: Representative immunofluorescence images show siCTL- or siBMPR2-treated huPASMC stimulated by S1P (1 µMol/L) or vehicle and transfected with a SMAD3-Myc plasmid stained for F-actin by phalloidin alone (left; green) or (right) in combination with anti-SMAD3 staining for SMAD3 (red) and diamidino-2-phenylindole (DAPI; blue). SMAD3-overexpressing cells are outlined by dotted lines. Representative images and quantitative analysis of mean phalloidin fluorescence intensity in SMAD3-overexpressing as compared to adjacent non-transfected cells show reduced formation of actin stress fibers in SMAD3-overexpressing cells at rest, after stimulation with S1P or *BMPR2* silencing, or a combination of both (replicated in n=3 independent experiments each). **P*<0.05 vs siCTL; #P<0.05 vs siCTLplasmid group; One-way ANOVA was applied with Tukey´s post-hoc test.

Figure 11: Schematic of proposed signalling pathway.

Short term and long term (chronic) effects of TGF-β stimulation on pulmonary artery smooth muscle cells. Initially, TGF-β signaling via the classic SMAD2/3 signaling axis

predominates, resulting in expression of SMAD3-dependent target genes but antagonizing TGF-β induced MRTF activation by SMAD3-MRTF interaction. Chronic TGF-β stimulation, however, leads to downregulation of SMAD3 (red dotted line) and therefore, reduced expression of SMAD3-dependent target genes. Functional loss of BMPR-II receptor signaling due to *BMPR2* mutations or receptor downregulation, respectively, replicates this effect, presumably in part by increasing TGF-β expression. Loss of SMAD3 then stimulates cell proliferation and migration in an MRTF-independent manner and concomitantly disinhibits MRTF (indicated by red cross) allowing MRTF to translocate into the nucleus and together with serum response factor (SRF) drive the SMA promoter, thus promoting both hypertrophy and hyperplasia in parallel.

A PAH (human)

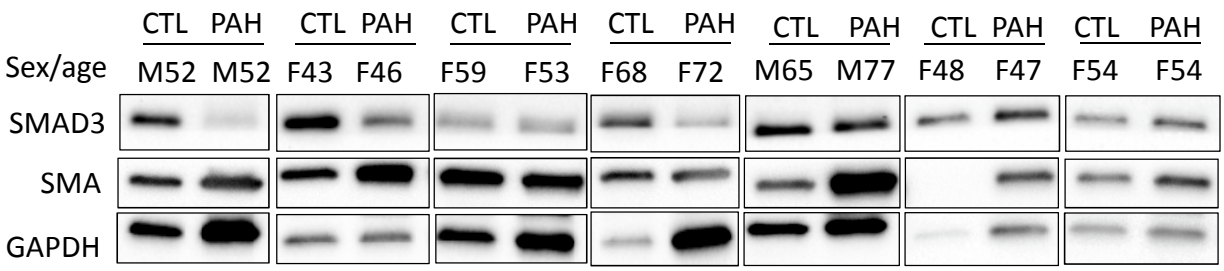

B

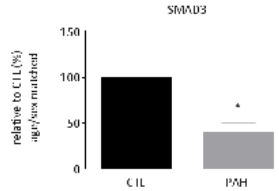

C

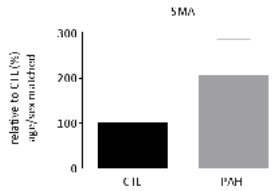

D MCT

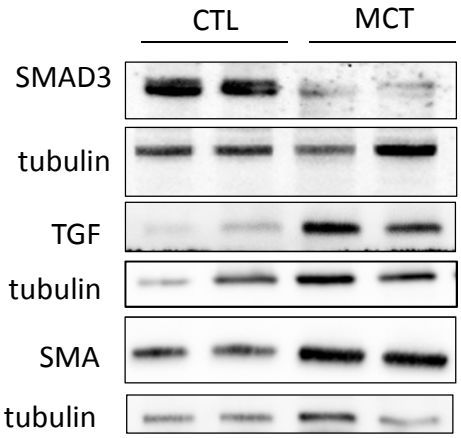

E

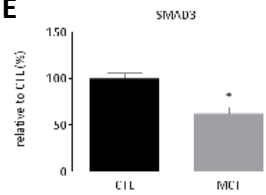

F

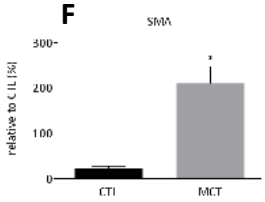

G

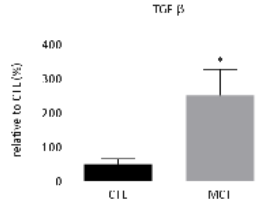

H

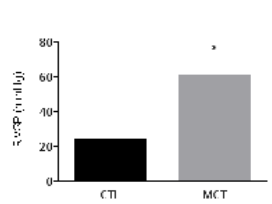

I Sugen/hypoxia

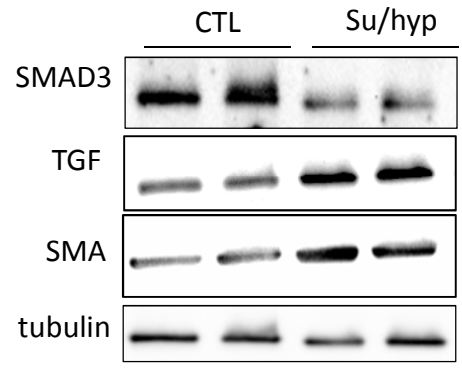

J

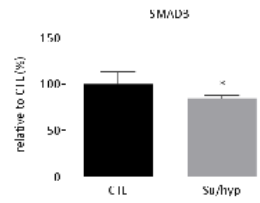

K

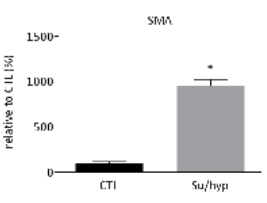

L

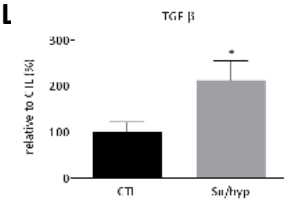

M

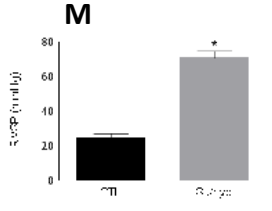

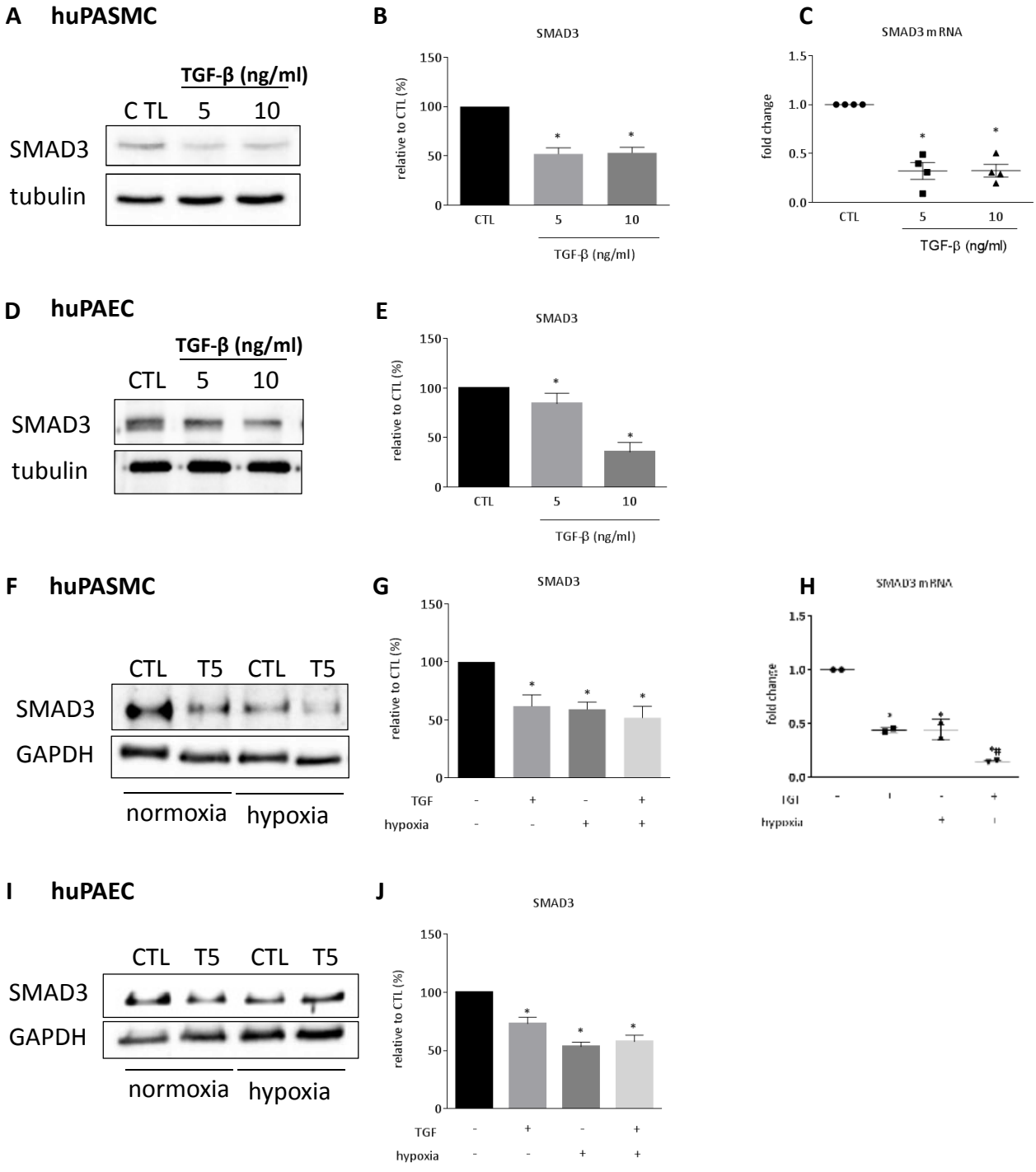
A huPASMC
TGF-β (ng/ml)
C TL 5 10
SMAD3
tubulin
B
SMAD3
relative to CTL (%)
CTL 5 10
TGF-β (ng/ml)
C
SMAD3 mRNA
fold change
CTL 5 10
TGF-β (ng/ml)
D huPAEC
TGF-β (ng/ml)
CTL 5 10
SMAD3
tubulin
E
SMAD3
relative to CTL (%)
CTL 5 10
TGF-β (ng/ml)
F huPASMC
CTL T5 CTL T5
SMAD3
GAPDH
normoxia hypoxia
G
SMAD3
relative to CTL (%)
TGF
hypoxia
H
SMAD3 mRNA
fold change
I huPAEC
CTL T5 CTL T5
SMAD3
GAPDH
normoxia hypoxia
J
SMAD3
relative to CTL (%)
TGF
hypoxia

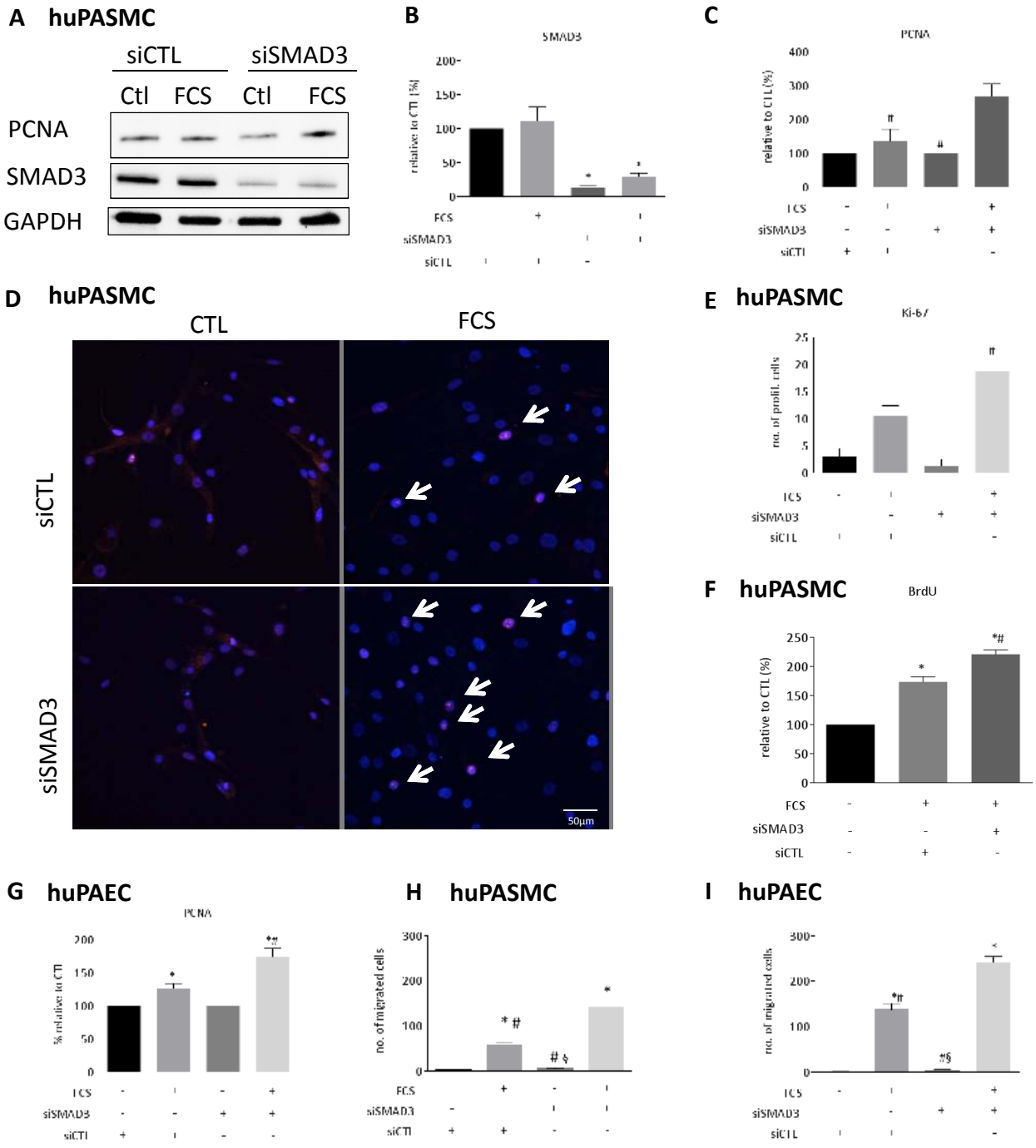
A huPASMC
siCTL
siSMAD3
Ctl
FCS
Ctl
FCS
PCNA
SMAD3
GAPDH
B
SMAD3
relative to CTL (%)
FCS
siSMAD3
siCTL
C
PCNA
relative to CTL (%)
FCS
siSMAD3
siCTL
D huPASMC
CTL
FCS
siCTL
siSMAD3
50µm
E huPASMC
Ki-67
no. of prolif. cells
FCS
siSMAD3
siCTL
F huPASMC
BrdU
relative to CTL (%)
FCS
siSMAD3
siCTL
G huPAEC
PCNA
% relative to CTL
FCS
siSMAD3
siCTL
H huPASMC
no. of migrated cells
FCS
siSMAD3
siCTL
I huPAEC
no. of migrated cells
FCS
siSMAD3
siCTL

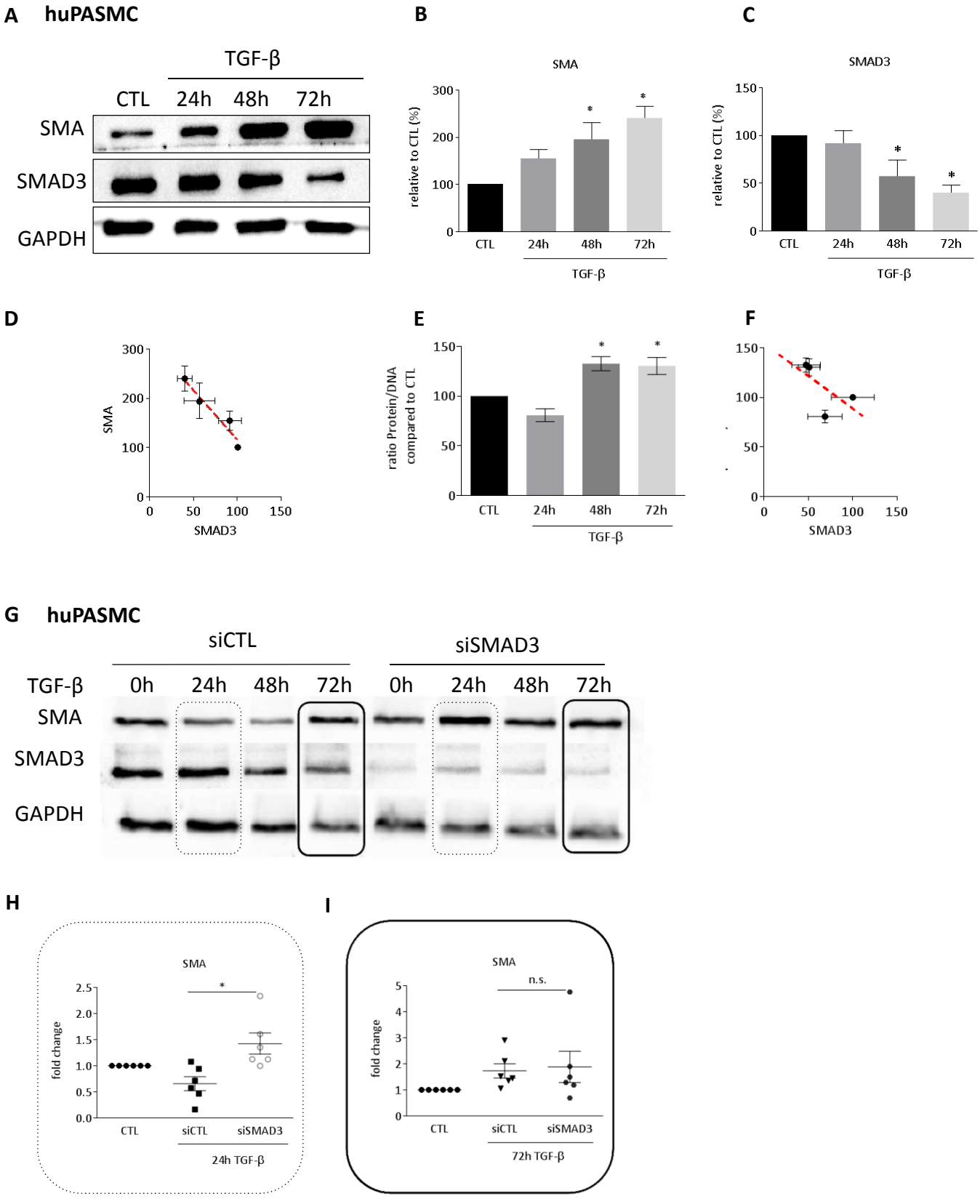
A huPASMC
TGF-β
CTL 24h 48h 72h
SMA
SMAD3
GAPDH
B
SMA
relative to CTL (%)
CTL 24h 48h 72h
TGF-β
C
SMAD3
relative to CTL (%)
CTL 24h 48h 72h
TGF-β
D
SMA
SMAD3
E
ratio Protein/DNA compared to CTL
CTL 24h 48h 72h
TGF-β
F
SMAD3
G huPASMC
siCTL
siSMAD3
TGF-β 0h 24h 48h 72h 0h 24h 48h 72h
SMA
SMAD3
GAPDH
H
SMA
fold change
CTL siCTL siSMAD3
24h TGF-β
I
SMA
n.s.
fold change
CTL siCTL siSMAD3
72h TGF-β

A huPASMC

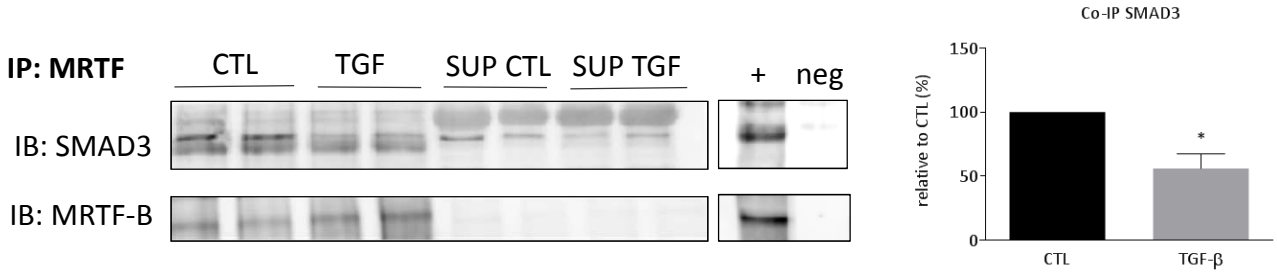

B huPASMC

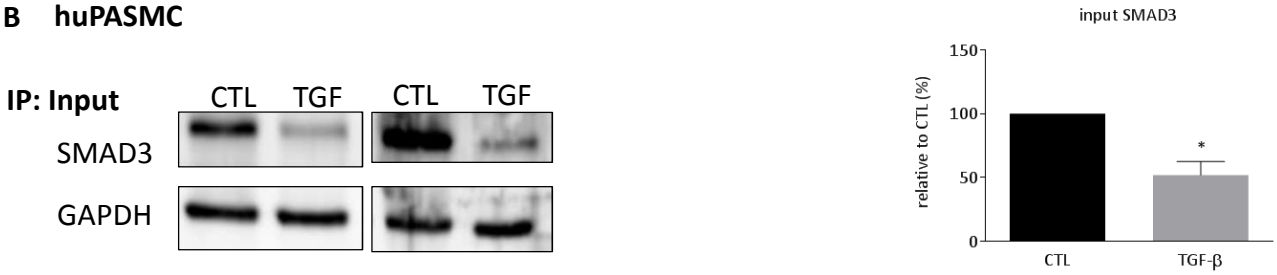

C MCT

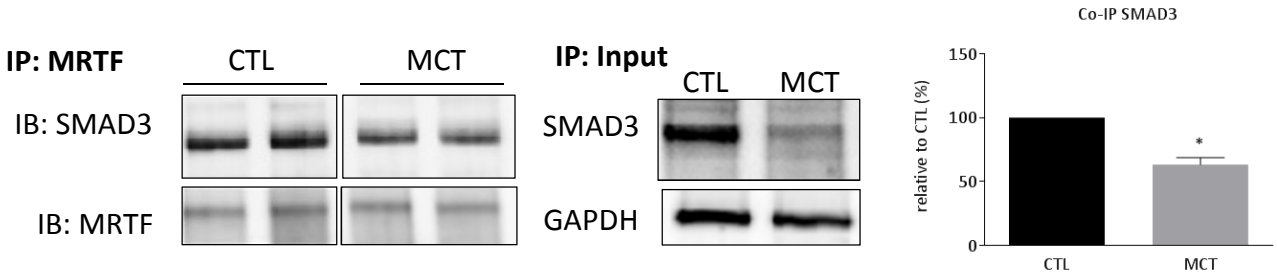

D Sugen/hypoxia

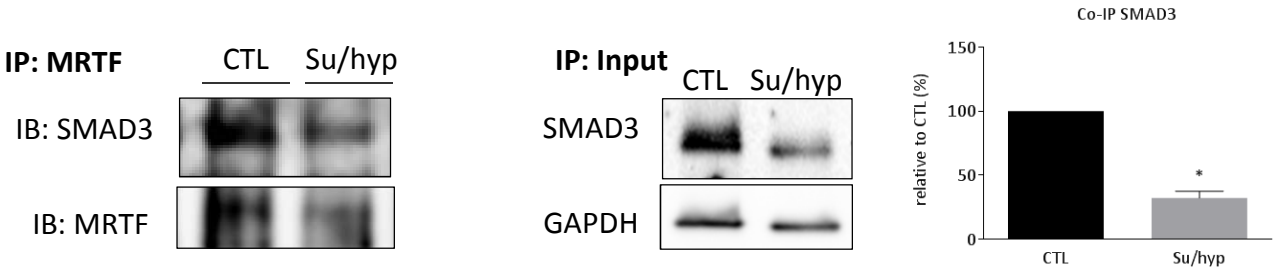

A huPASMC

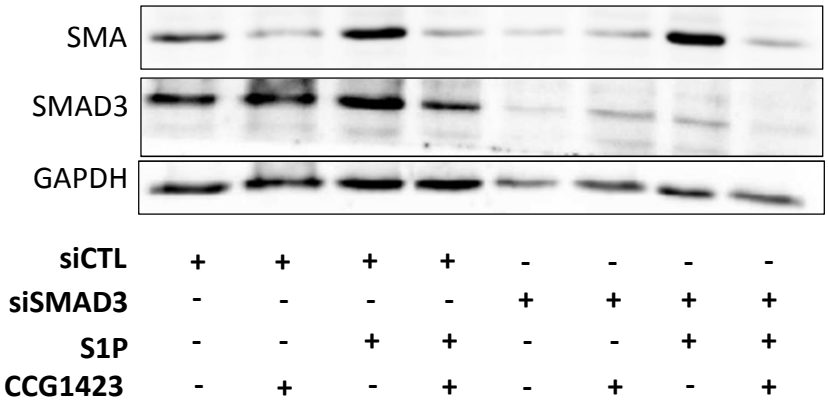

B

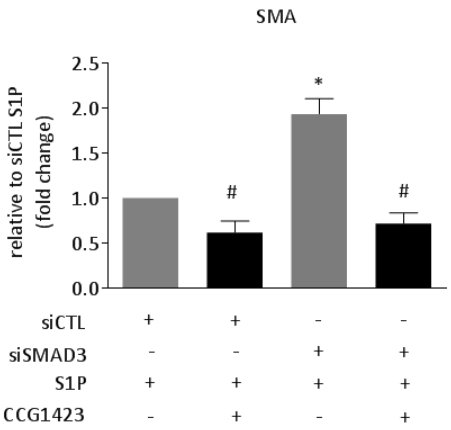

C huPASMC

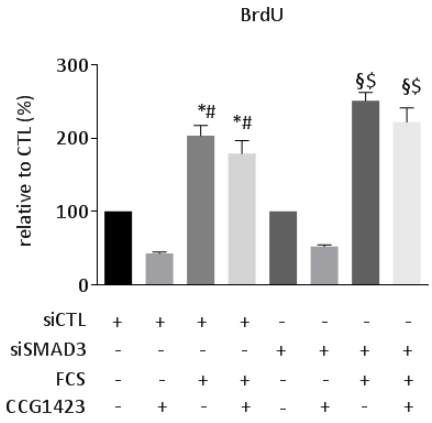

D huPAEC

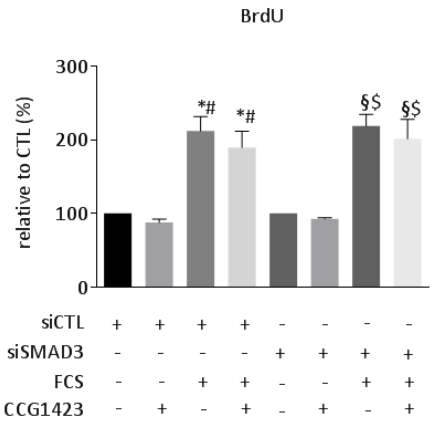

E huPASMC

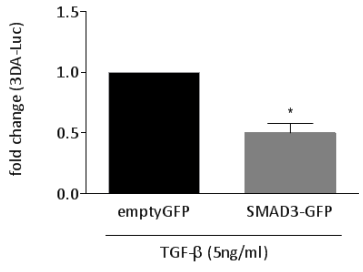

F huPASMC

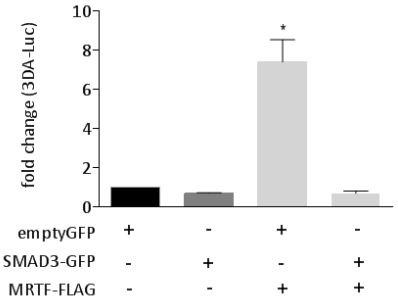

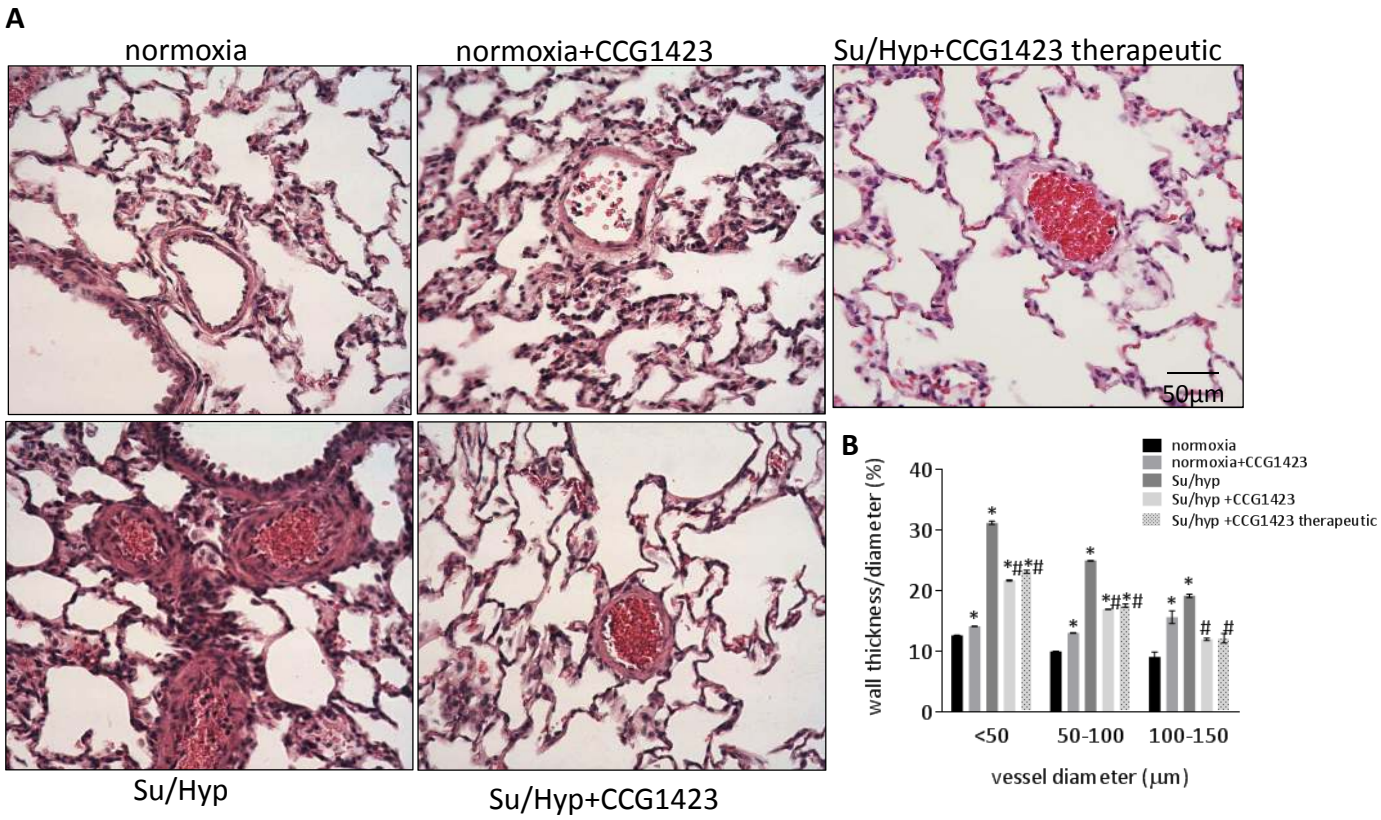
A
normoxia
normoxia+CCG1423
Su/Hyp+CCG1423 therapeutic
50µm
Su/Hyp
Su/Hyp+CCG1423
B
normoxia
normoxia+CCG1423
Su/hyp
Su/hyp +CCG1423
Su/hyp +CCG1423 therapeutic
wall thickness/diameter (%)
<50
50-100
100-150
vessel diameter (µm)

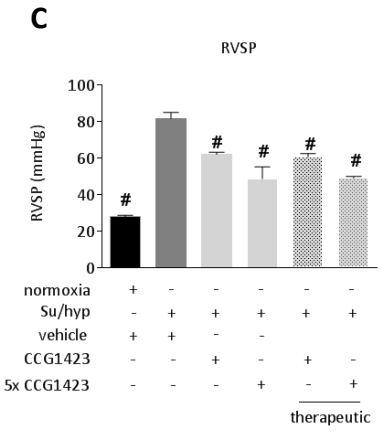
C
RVSP
RVSP (mmHg)
normoxia
Su/hyp
vehicle
CCG1423
5x CCG1423
therapeutic

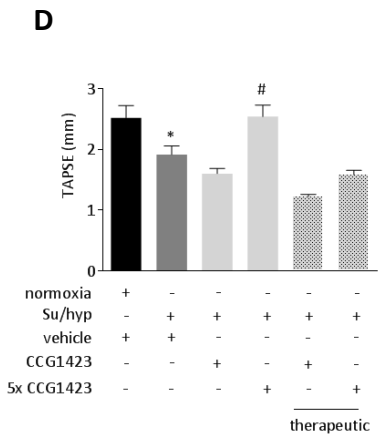
D
TAPSE (mm)
normoxia
Su/hyp
vehicle
CCG1423
5x CCG1423
therapeutic

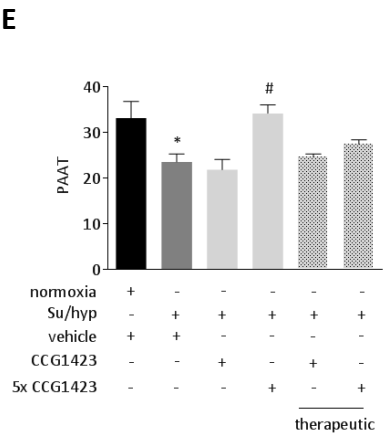
E
PAAT
normoxia
Su/hyp
vehicle
CCG1423
5x CCG1423
therapeutic

A

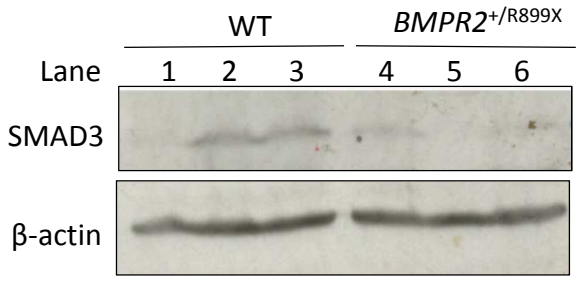
WT
BMPR2+/R899X
Lane
1 2 3 4 5 6
SMAD3
β-actin

B

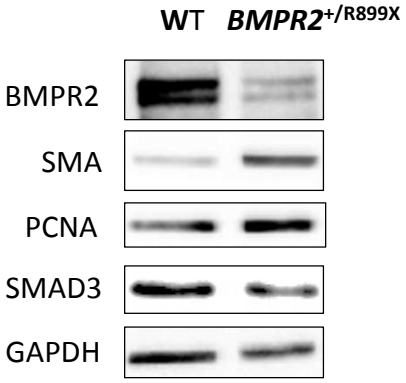
WT
BMPR2+/R899X
BMPR2
SMA
PCNA
SMAD3
GAPDH

C

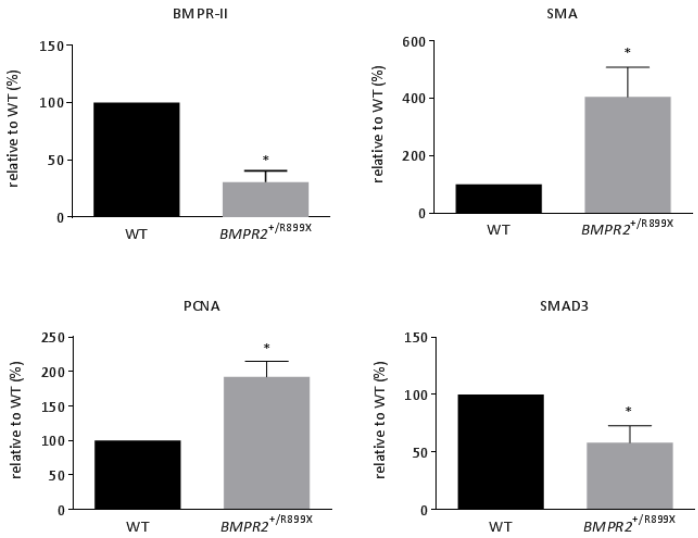
BMPR-II
SMA
PCNA
SMAD3
relative to WT (%)
WT
BMPR2+/R899X
*

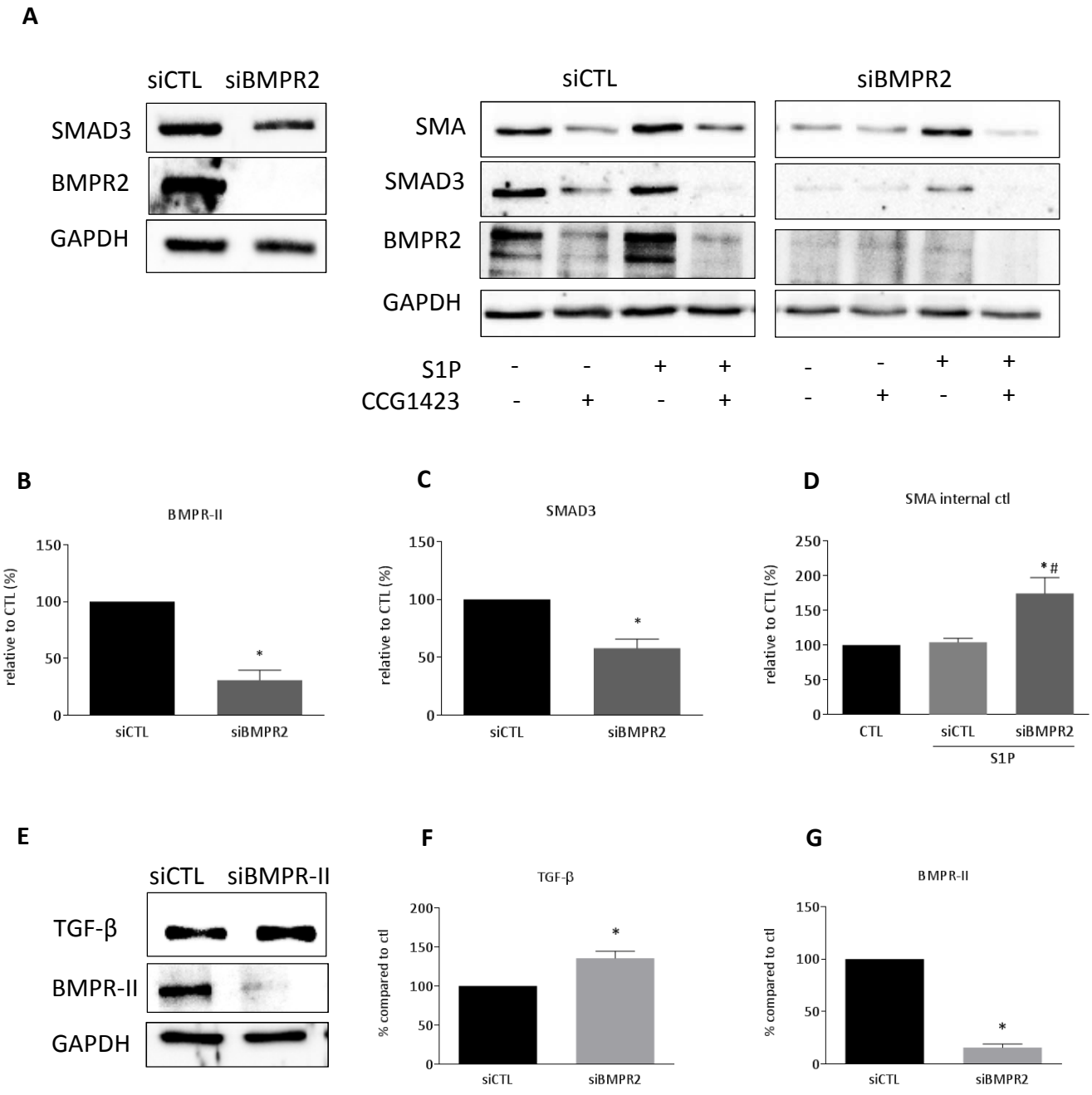
A
siCTL
siBMPR2
SMAD3
BMPR2
GAPDH
siCTL
siBMPR2
SMA
SMAD3
BMPR2
GAPDH
S1P
CCG1423
B
BMPR-II
relative to CTL (%)
siCTL
siBMPR2
C
SMAD3
relative to CTL (%)
siCTL
siBMPR2
D
SMA internal ctl
relative to CTL (%)
CTL
siCTL
siBMPR2
S1P
E
siCTL
siBMPR-II
TGF-β
BMPR-II
GAPDH
F
TGF-β
% compared to ctl
siCTL
siBMPR2
G
BMPR-II
% compared to ctl
siCTL
siBMPR2

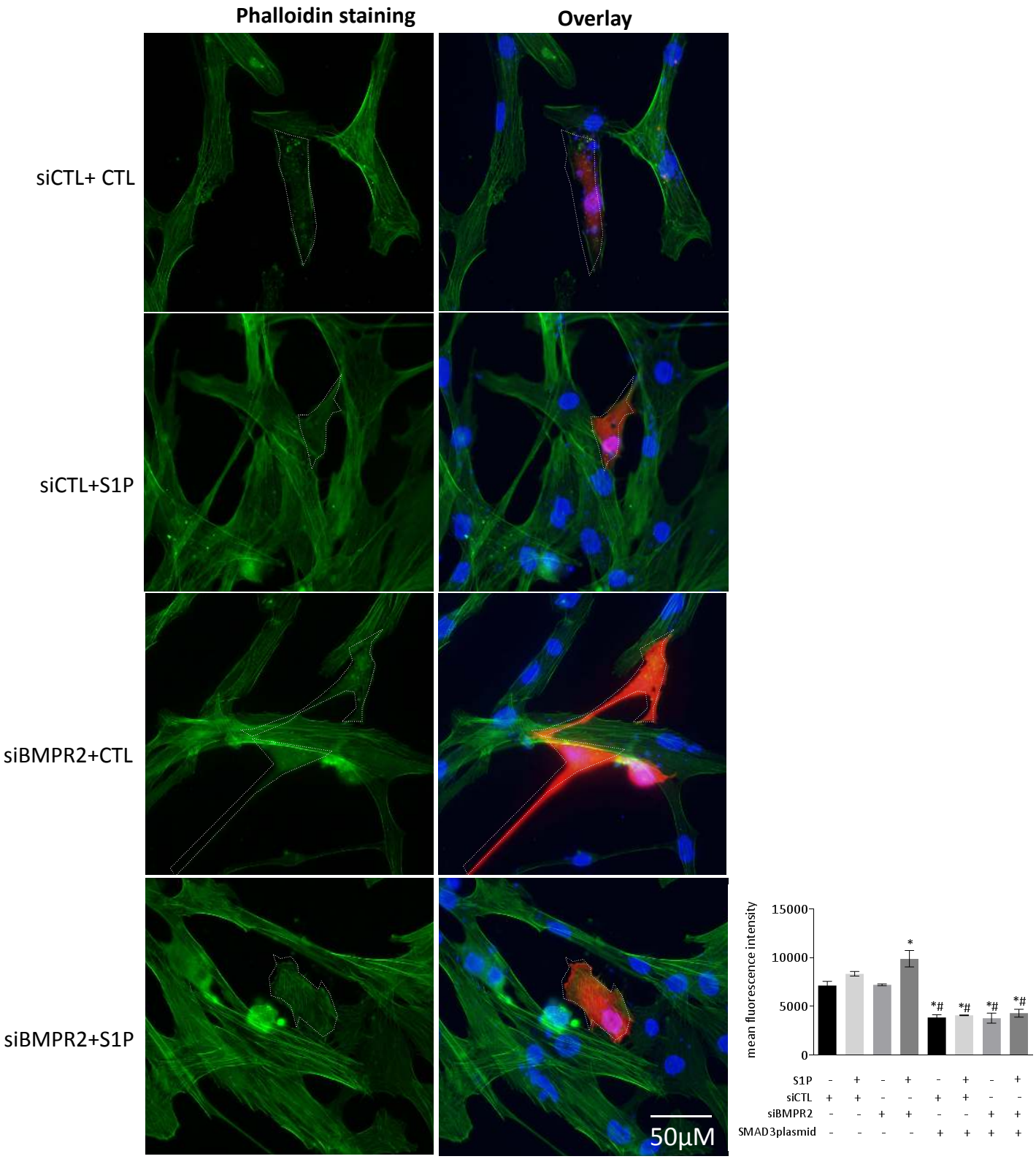
Phalloidin staining
Overlay
siCTL+ CTL
siCTL+S1P
siBMPR2+CTL
siBMPR2+S1P
50µM
mean fluorescence intensity
15000
10000
5000
0
*
*#
*#
*#
S1P - + - + - + - +
siCTL + + - - + + - -
siBMPR2 - - + + - - + +
SMAD3plasmid - - - - + + + +

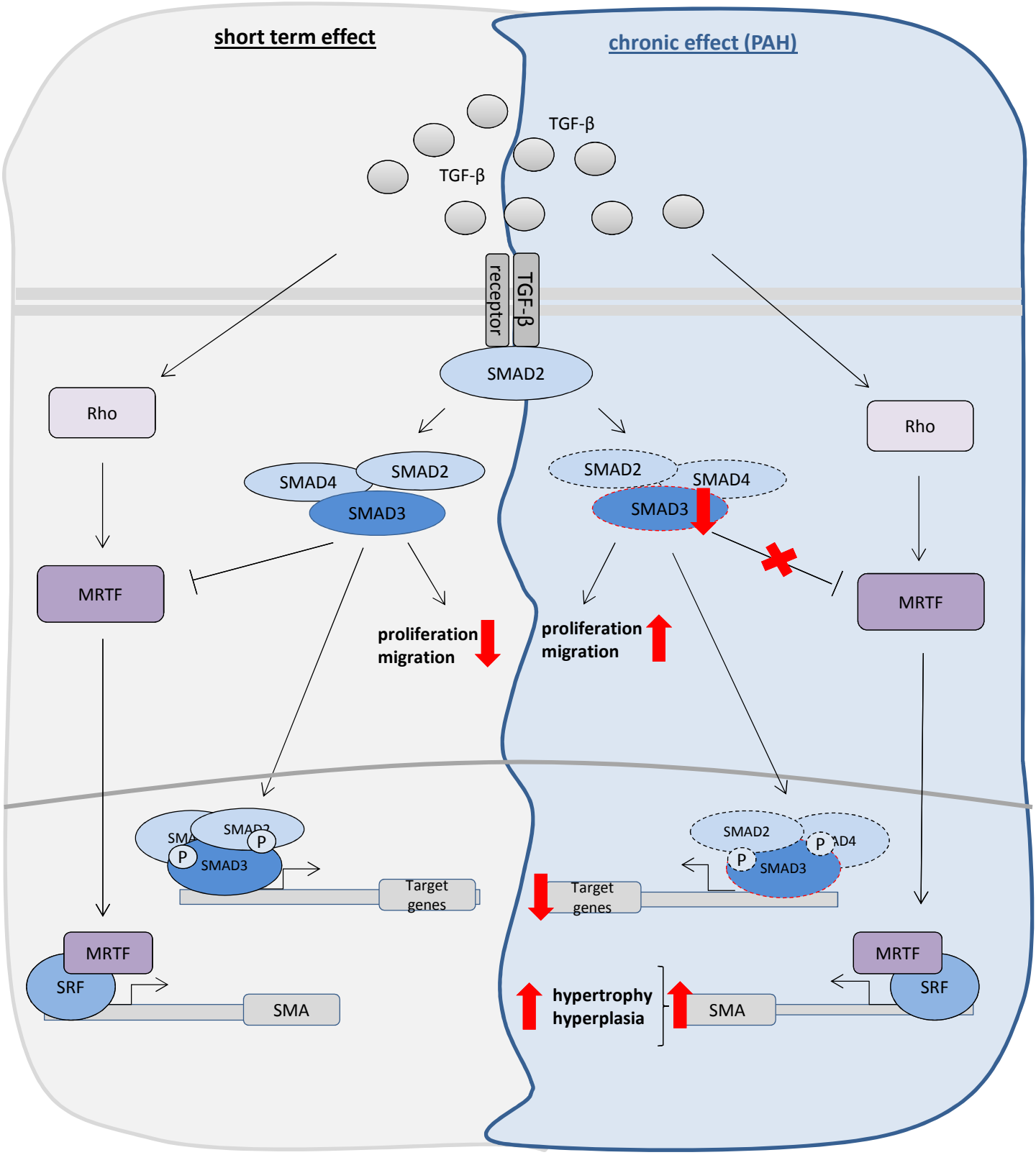
short term effect
chronic effect (PAH)
TGF-β
TGF-β
receptor
TGF-β
SMAD2
Rho
Rho
SMAD4
SMAD2
SMAD3
SMAD2
SMAD4
SMAD3
MRTF
MRTF
proliferation
migration
proliferation
migration
SMAD2
P
P
SMAD3
SMAD2
P
P
SMAD3
Target genes
Target genes
MRTF
SRF
SMA
MRTF
SRF
SMA
hypertrophy
hyperplasia

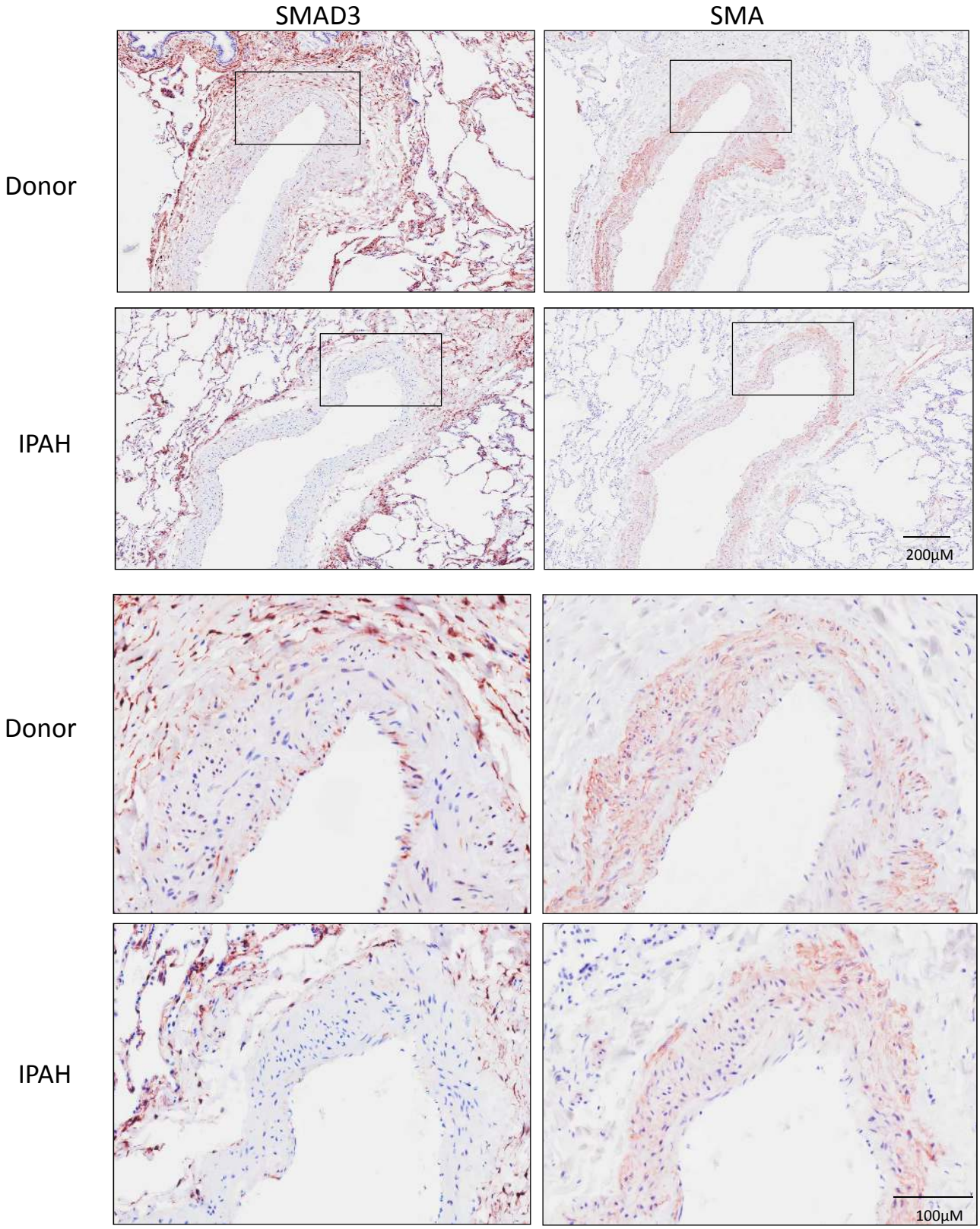
SMAD3
SMA
Donor
IPAH
200µM
Donor
IPAH
100µM

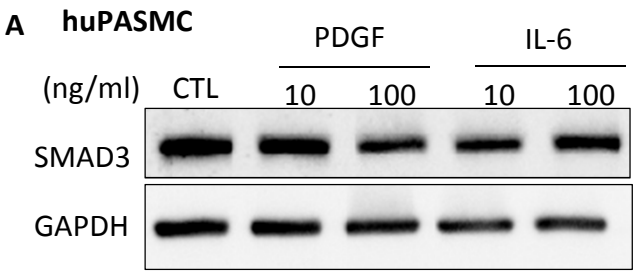
A
huPASMC
PDGF
IL-6
(ng/ml)
CTL
10
100
10
100
SMAD3
GAPDH

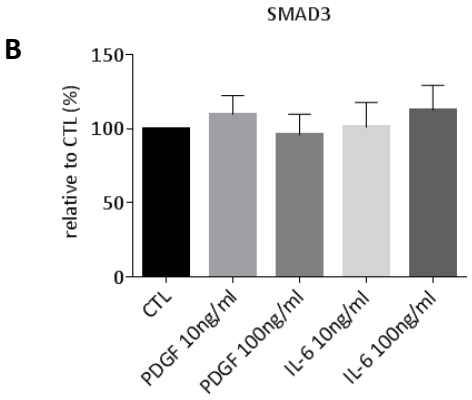
B
SMAD3
relative to CTL (%)
150
100
50
0
CTL
PDGF 10ng/ml
PDGF 100ng/ml
IL-6 10ng/ml
IL-6 100ng/ml

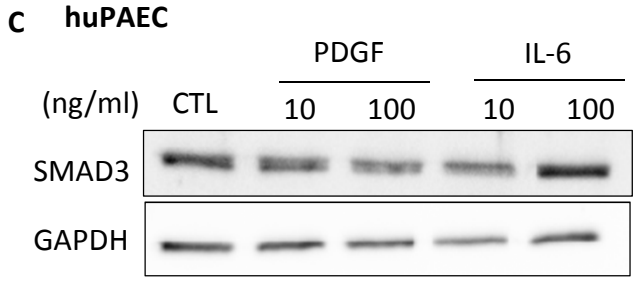
C
huPAEC
PDGF
IL-6
(ng/ml)
CTL
10
100
10
100
SMAD3
GAPDH

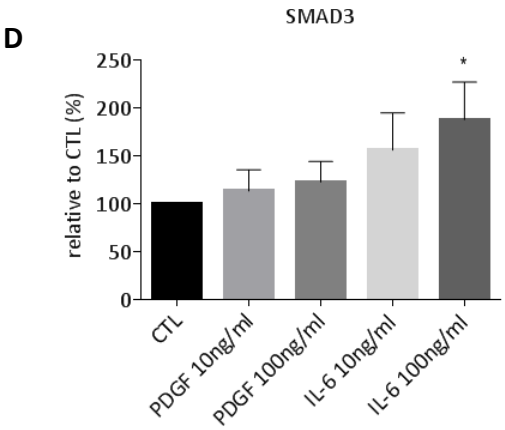
D
SMAD3
relative to CTL (%)
250
200
150
100
50
0
*
CTL
PDGF 10ng/ml
PDGF 100ng/ml
IL-6 10ng/ml
IL-6 100ng/ml

A huPASMC activated Caspase 3

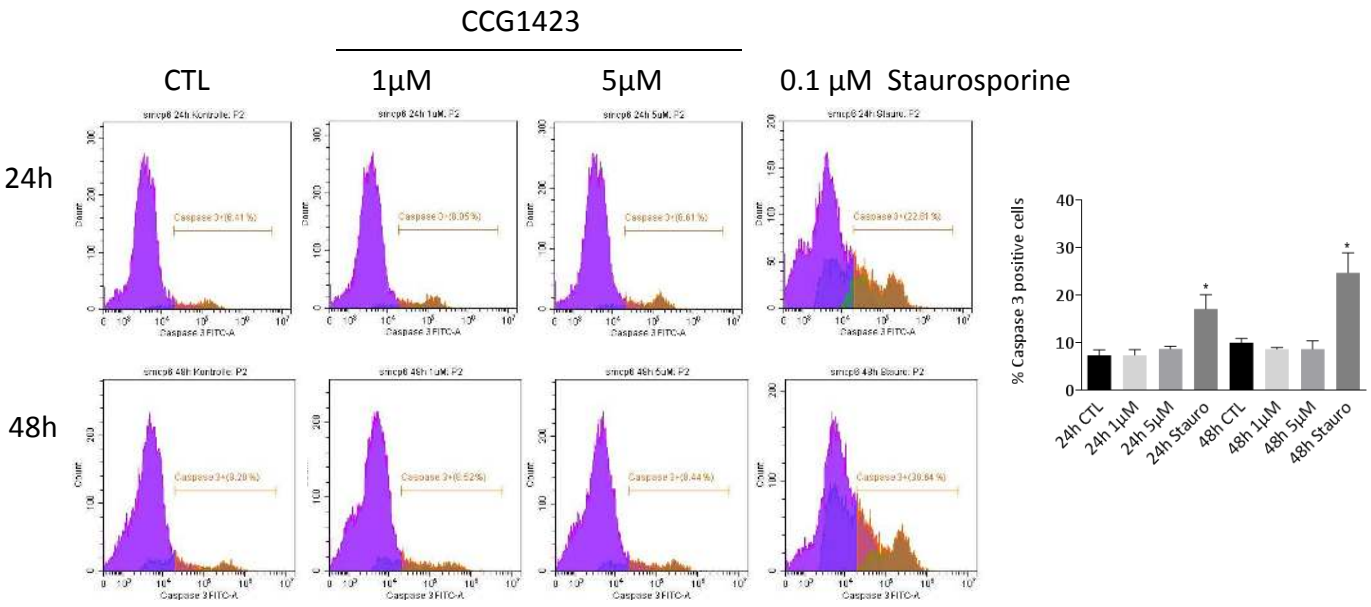

B huPAEC activated Caspase 3

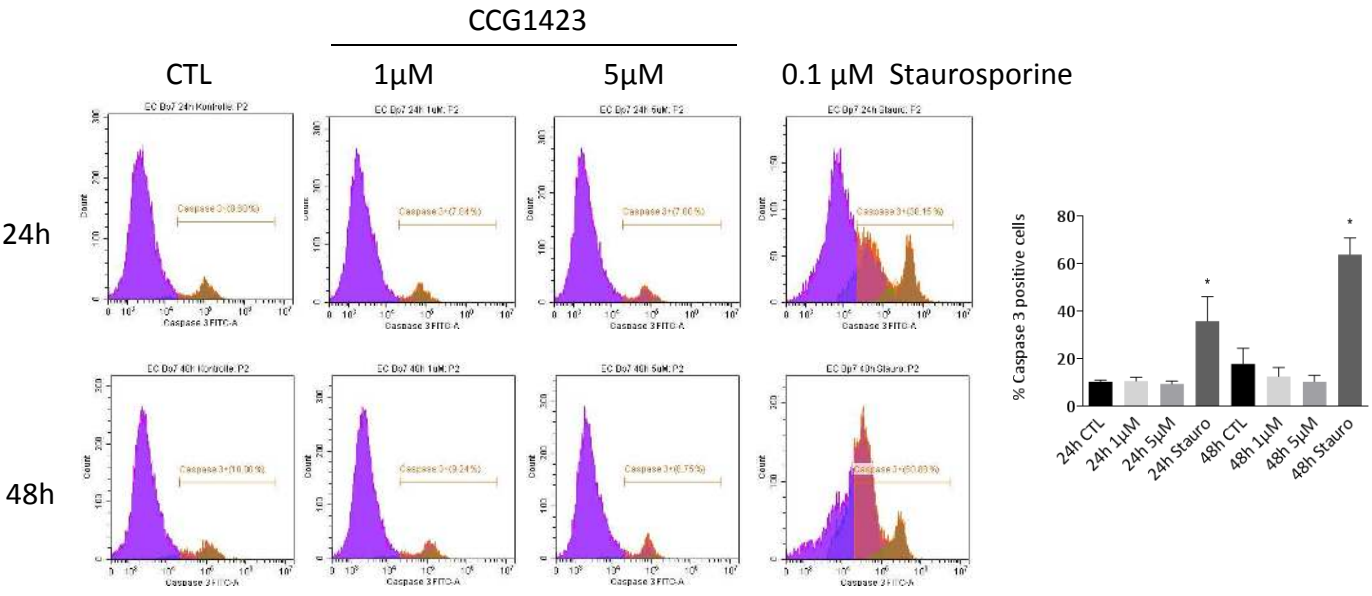

A huPASMC

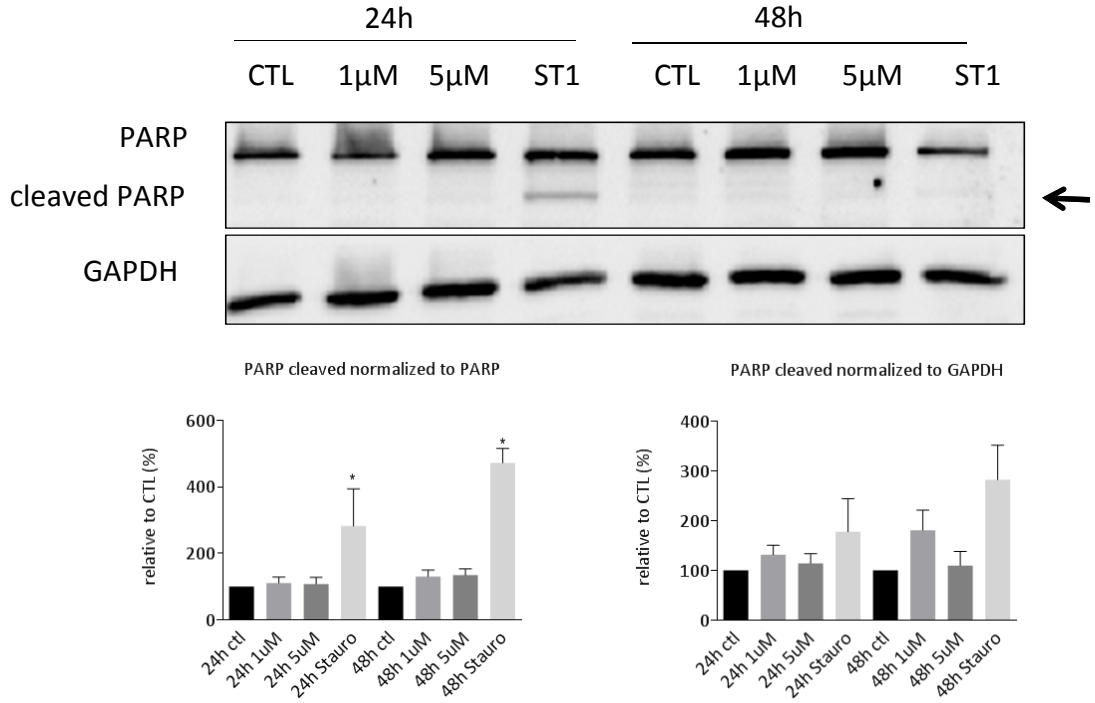

B huPAEC

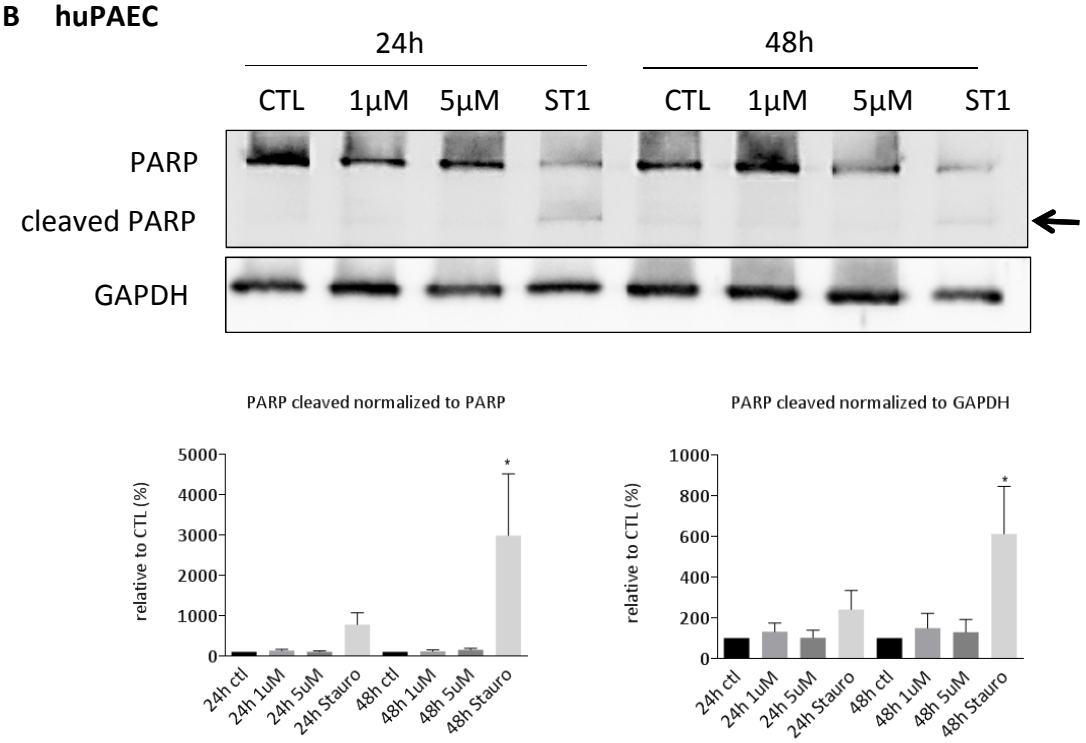

huPASMC

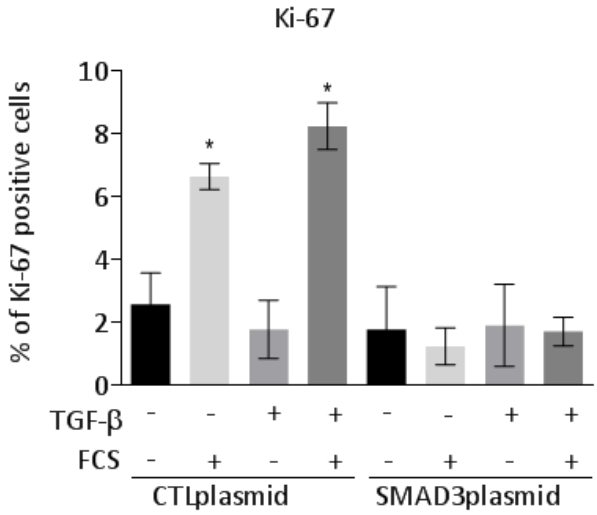
Ki-67
% of Ki-67 positive cells
10
8
6
4
2
0
*
*
TGF-β - - + + - - + +
FCS - + - + - + - +
CTLplasmid
SMAD3plasmid

A

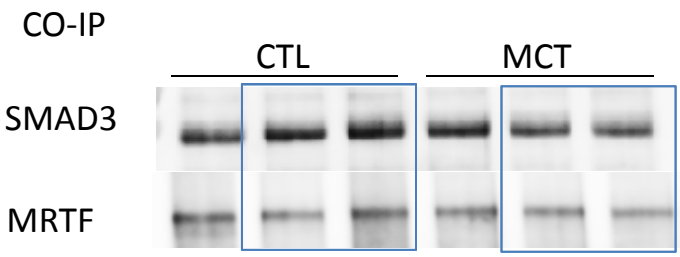
CO-IP
CTL
MCT
SMAD3
MRTF

B

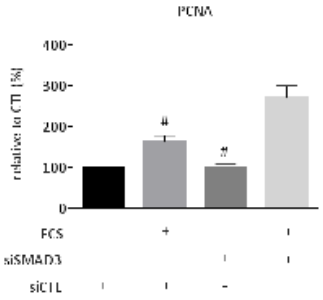
PCNA
400
300
200
100
0
#
#
FCS
+
siSMAD3
siCTL

Online Supplement

Methods

Cells. Human pulmonary arterial smooth muscle cells (huPASMC) and human pulmonary arterial endothelial cells (huPAEC) purchased from Promocell (C-12521, Heidelberg, Germany) and Lonza (CC-2530, Basel, Switzerland), respectively, were cultured either in Smooth Muscle (C-22062) or Endothelial Cell Growth Medium 2 (C-22211) both purchased from Promocel and used from passage 4-8. Murine PASMC were obtained from *BMPR2*$^{+/R899X}$ mice which carry a mutated allele of the *BMPR2* gene, and corresponding wild type mice as previously described [1], and cultured in Smooth Muscle Growth Medium 2 (Promocell).

Protein isolation and western blotting. For protein extraction, human (donor and PAH) as well as rat lung samples (normoxic, SU5416/hypoxia as well as MCT treated rats) were ground in liquid nitrogen. HuPASMC or huPAEC were lysed in RIPA buffer with protease inhibitor complex and phosphatase inhibitors (Roche, Basel, Switzerland). After incubation on ice for 30 minutes, samples were centrifuged (12,000g, 10 min, 4°C), and the protein concentration in the supernatant was determined by spectrophotometry (BCA assay, Pierce, Rockford, IL, USA). Final concentrations of 10 µg of protein were run on a 10% sodium dodecyl sulfate (SDS) polyacrylamide gel, followed by electrotransfer to a 0.2-µm pore nitrocellulose membrane (Bio-Rad, Bio-Rad Laboratories, Mississauga, Ontario, Canada). After blocking with 5% non-fat dry milk in TBS-T buffer (Tris-buffered saline with 0.1% Tween20), the following antibodies were applied over night at 4°C: SMAD3 (1:1000; #9523S; Cell Signaling Technology, Danvers, MA, USA), MRTF-B (1:2000; sc61074; Santa Cruz Biotechnology, Dallas, Texas, USA), SMA (1:10000; A2547; Sigma Aldrich), PCNA (1:2000; #2586S; Cell Signaling Technology, Danvers, MA, USA), BMPR-II (1:1000; 612292; BD Biosciences, Mississauga, ON, Canada); TGF-β (1:2000; ab179695; Abcam;

Cambridge, United Kingdom); PARP (1:1000; #9542; Cell Signaling Technology, Danvers, MA, USA); GAPDH (1:5000; sc25778; Santa Cruz Biotechnology, Dallas, Texas, USA), tubulin (1:10000; #2125S; Cell Signaling Technology, Danvers, MA, USA). Secondary antibodies were purchased from Jackson ImmunoResearch and applied at a 1:5000 dilution. Final detection of proteins was performed using the Amersham ECL Prime Western Blotting Detection System (GE Healthcare, Wien, Austria).

Transfection. Pre-designed, commercially available siRNA sequences directed against human SMAD3 and BMPR2 were purchased (Dharmacon Thermo Sientific). For non-specific gene inhibition of the siRNAs used in this study, a universal negative-control siRNA sequence was used (Dharmacon Thermo Sientific). For SMAD3 overexpression a GFP-tagged Smad3 from cClonetech or a Myc-tagged Smad3 expression constructs (in pCMV5B) was used which was a kind gift from L. Attisano (University of Toronto).) , for MRTF overexpression a FLAG-tagged MRTF construct kindly provided by E.N. Olsen (University of Texas, Southwestern Medical Center, Dallas, TX) . Cells were transfected with 100nMol/L siRNA or 0.5-2µg plasmid for 8h using Effectene, Transfection Reagent (Qiagen, Toronto, Ontario, Canada) .

Proliferation assays. For SMAD3 silencing, huPASMCs or huPAECs were treated for 8 h with SMAD3-specific (siSMAD3) or scrambled (siCTL) small interference RNA (100nMol/L L-020067-00-0005 or D-001810-10-05, respectively; Dharmacon Thermo Scientific)). Tenthousand cells per well were seeded on 96 well plates and kept overnight in starvation medium (0% FCS). The following day cells were stimulated with basal media with or without 5% FCS and or 5 µMol/L CCG1423 (10010350**;** Cayman Chemical, Ann Arbor, Michigan; USA). Proliferation of huPASMCs and huPAECs was determined by immunoblotting for proliferating cell nuclear antigen (PCNA #2586, Cell Signaling Technology, Danvers, MA, USA), by incorporation of bromodeoxyuridine (BrdU assay) according to manufacturer

instructions (#6813**;** Cell Signaling Technology, Danvers, MA, USA), or by immunocytochemical staining for Ki-67, respectively.

Migration assay. huPASMCs and huPAECs were treated with siSMAD3 or siCTL as described above. The next day, 20,000 cells per 24-transwell (CA62406-198; VWR, Mississauga, Ontario, Canada) were seeded and allowed to migrate towards basal medium with or without 5% FCS for 6h. Cells were fixed with ice-cold methanol and stained with haematoxylin. Residual non-migrated cells in the compartment of the transwell were removed and migrated cells on the lower filter insert were counted manually.

RNA isolation and real-time PCR. Total cellular RNA was isolated from huPASMCs and huPAECs by use of the RNeasy Mini Kit from Qiagen (Toronto, Ontario, Canada). A Nanodrop 2000c spectrophotometer (PeQlab) was used to quantify the concentration and the purity of the isolated total RNA. Total RNA was reverse transcribed to cDNA using an iScript™ cDNA Synthesis Kit (Bio-Rad, Mississauga, Ontario) and amplified using a Lightcycler 480 (Roche, Basel, Switzerland). The PCR reactions were performed with QuantiFast SYBR PCR kit (Qiagen, Toronto, Ontario, Canada). Gene expressions were calculated using the ΔCt method with GAPDH serving as control.

Co-immunoprecipitation. Cell lysates of TGF-β (5 ng/mL for 72 h) or vehicle treated huPASMCs, or pulmonary arteries isolated from MCT, Sugen-hypoxia, or control rats were incubated with an antibody directed against MRTF-B (1:100; Santa Cruz Biotechnology, Dallas, Texas, USA) over night at 4°C. To collect the formed complex composed of anti-MRTF-B antibody bound to MRTF-B and possible binding partners (SMAD3), protein G (or A) sepharose was added the next day for 1h at 4°C. After centrifugation (3-5 min at 2,000 rpm at 4°C) and 5x washing with cell lysis buffer, the supernatant of the sample was carefully

removed and 2x concentrated SDS-PAGE sample loading buffer with denaturising β-mercaptoethanol was added to the pellet. The samples were boiled at 95°C for 10 min and western blots for SMAD3 (1:1000; Cell Signaling Technology, Danvers, MA, USA) and MRTF-B (1:2000; Santa Cruz Biotechnology, Dallas, Texas, USA) protein levels were performed on the immunoprecipitated pellet, as well as the supernatant and the original input (cell lysate) as corresponding controls.

Immunocytochemistry. Cells were fixed with 4% methanol-free paraformaldehyde and treated for 10 min with 100 mMol/L glycerol followed by 15 min of 0.1% TritonX100 (Sigma). After 1h 5% treatment with bovine serum albumin (BSA) cells were stained with anti-SMAD3 (1:100; Cell Signaling Technology, Danvers, MA, USA) for 1h at room temperature. Alexa Fluor555 donkey-anti-rabbit (1:200; Thermo Fisher Scientific) was applied as secondary antibody. For actin staining Alexa Fluor Phalloidin488 (1:100; Thermo Fisher Scientific) was applied for 1h at room temperature. Mounting medium with DAPI was used from Vectorshield, Burlingame, Canada.. Pictures were taken with an Nikon Upright E800 microscope.

Immunohistochemistry. Serial cut human lung slides from donor or IPAH patients were deparaffinized and stained for SMAD3 (1:100, #9523S; Cell Signaling Technology, Danvers, MA, USA) or SMA (1:300, A2547; Sigma Aldrich) overnight in 4°C; secondary antibody staining was performed with the Vektor ImmPRESS reagent kit (Vector Laboratories Ltd, Peterborough, UK). Hematoxylin was applied for counterstaining.

Flow cytometry: For caspase-3 analysis, cells were treated either with 1µMol/L or 5µMol/L CCG1423 for 24h or 48h. Staurosporine (0.1µMol/L) served as positive control. Cells and supernatant were collected, centrifuged and washed with PBS. For caspase 3 staining the

CellEvent™ Caspase-3/7 Green Flow Cytometry Assay Kit was employed according to the manufacturer´s instructions (C10427; Life Technologies, Carlsbad, CA), and caspase-3 positive events were detected and analysed on a CytoFLEX using CytExpert software (Beckman Coulter Life Sciences, Indianapolis, IN). For Ki-67 analysis, cells were fixed in 1% parafomraldehyde (PFA) for 15min on ice. After 15min treatment with 0.3% saponin and subsequent PBS washing steps, cells were stained for 20min with a Ki-67 phycoerythrin-labeled antibody (Ki-67 PE set, Becton Dickinson, Vienna, Austria), and analyzed on a LSRII cytometer (Becton Dickinson, Franklin Lakes, NJ, USA, State).

Luciferase Reporter Assays: Assays were carried out as described previously ([2]). Briefly, 70 – 80% confluent PASMCs were incubated in 0% serum for 2 hr and then co-transfected using 0.6 µL/mL of Human Artery Smooth Muscle Cell Avalanche (EZ Biosystems, LLC) according to manufacturer's instructions. Cells were co-transfected with the MRTF/SRF sensitive promoter plasmid pGL3-3DA-Luc (0.25 µg/mL) which contains the firefly luciferase gene under the control of a CArG box triplet, the control plasmid pRL-TK (0.05 µg/mL), and one of the following four constructs: empty GFP (0.5 – 2 µg, Clonetech, Mountain View, CA ,USA), GFP-Smad3 (0.5 – 2 µg, Clonetech), pcDNA (0.1 µg, Invitrogen, Burlington, ON, Canada), FLAG-MRTFB (0.1 µg, kindly provided by E.N. Olsen, Univ. of Texas Southwestern Medical Center, Dallas, TX). Cells were treated 24h later as described for individual experiments and lysed on ice with 1x Passive Lysis Buffer (Promega, Madison, WI, USA). The luciferase assay was conducted using the Dual Luciferase Kit (Promega) as per manufacturer's instructions.

Pulmonary hypertension models. The study was approved by the animal care and use committee of St. Michael´s (ACC #554), and all experiments were performed in accordance with the "Guide for the Care and Use of Laboratory Animals" (Institute of Laboratory Animal Resources, 7th edition 1996).

Sugen-hypoxia model: Male Sprague-Dawley (Charles River Laboratories, St. Constant, QC) rats with a starting body weight (bw) of 200g received a single subcutaneous injection of the VEGF receptor antagonist SU5416 (20 mg/kg bw dissolved in 0.5% carboxymethylcellulose sodium + 0.9% sodium chloride + 0.4% Tween80 + 0.9% benzyl alcohol in distilled water) and were subsequently exposed to 10% O_2 (hypoxia) for 3 weeks, followed by 2 weeks of normoxia (21% O_2) as previously described[3]. In subgroups of animals, the pharmacological MRTF inhibitor CCG1423 (0.15mg/kg or 0.75mg/kg [5xCCG1423] in DMSO, Cayman Chemicals, Ann Arbor, Michigan, USA) or respective vehicle was delivered daily via intraperitoneal injections either from day 0 (prophylactic approach) or from day 21 (therapeutic approach) after SU5416 injection.

Monocrotaline model: Male Sprague-Dawley rats (Charles River Laboratories, St. Constant, QC) with a starting bw of 200 g were treated with either a single intraperitoneal injection of monocrotaline (MCT; 60 mg/kg, Sigma, Deishofen, Germany in distilled water, pH: 7.5) or vehicle alone. After 21 days the animals underwent hemodynamic characterization (*vide infra*) and were sacrificed for organ harvesting.

Hemodynamic characterization. Rats were anesthetized by isoflurane inhalation (5%). Right ventricular systolic pressure (RVSP) measurements were performed as previously described [4] using a closed chest technique. Briefly, a 1.4 mm pressure catheter (Millar Instruments, Houston, TX, USA) was inserted into the jugular vein and directed to the right ventricle. Pressure recordings were made over a two minute period each and analyzed with Powerlab Pro software (AD Instruments Spechbach, Germany).

Echocardiographic imaging of right ventricular function was performed in anesthetized rats using a 12-MHz probe (Hewlett Packard Sonos 5500, Philips, Ultrasound, Bothell), and tricuspid anular plane systolic excursion (TAPSE) and pulmonary artery flow acceleration time (PA time) were quantified as surrogates for pulmonary hypertension.

Vascular remodelling. Hematoxylin and eosin staining was performed on paraffin fixed lung tissue slides. For quantification of medial wall thickness, external and internal (lumen) area as well as vessel diameter was determined for all pulmonary arteries within the field of observation, and the difference between external and internal vessel area relative to the external area was quantified. Vessels were categorized according to external diameter in <50 µm, 50-100 µm, and >100 µm pulmonary arteries.

Fulton Index. After exsanguination, lungs and hearts were isolated. The right ventricle (RV) was dissected from the left ventricle and septum (LV+S) and the samples were weighed separately to obtain the right-to-left ventricle plus septum weight ratio [RV/(LV+S); Fulton index] as a measure of right ventricular hypertrophy.

Statistical analysis. Statistical analyses were performed by use of GraphPad Prism software (GraphPad Prism 6.0; GraphPad Software Inc., La Jolla, CA). All data are presented as means ± SEMs. Student's t-test (two-tailed) was used to compare two groups. For >2 groups, two-way Analysis of Variance (ANOVA) was applied and Turkey was used as a post-hoc test. Linear regression analysis was performed by GraphPad Prism software. *P*-values < 0.05 were considered as statistically significant.

Supplementary Table 1: Clinical data of patient cohort given in mean+/- SEM

	Control	**PAH**
body mass index (kg/m^2)	26±2	22.8±4.7
WHO / NYHA	NA	III and IV
TVC (POD/RAP/PVC) (mmHg)	NA	13.5±5.4
systolic pulmonary arterial pressure (PAP) (mmHg)	NA	81±14.8
diastolic PAP (mmHg)	NA	33±4.2
mean PAP (mmHg)	NA	51±8.8
systolic blood pressure (mmHg)	NA	113±10.1
diastolic blood pressure (mmHg)	NA	69±6.6
mean blood pressure (mmHg)	NA	88±9.6
cardiac output (L/min)	NA	4±1.1
cardiac index (L/min/m^2)	NA	2±0.5
pulmonary capillary wedge pressure (mmHg)	NA	10±3.1
SvO_2 mixed venous oxygen saturation (%)	NA	56±10.7
heart rate (bpm)	NA	82±9.2
pulmonary vascular resistance (PVR) (dyne·s·cm^{-5})	NA	808±66.3
arterial oxygen saturation (SaO_2) (% at rest)	NA	91±2.8
6 min walk distance (m)	NA	281±101
arterial oxygen saturation (SaO_2) (% after 6min)	NA	81±7.7

References:

1. Han, C. *et al.* SMAD1 deficiency in either endothelial or smooth muscle cells can predispose mice to pulmonary hypertension. *Hypertension* **61,** 1044–52 (2013).
2. Speight, P., Kofler, M., Szászi, K. & Kapus, A. Context-dependent switch in chemo/mechanotransduction via multilevel crosstalk among cytoskeleton-regulated MRTF and TAZ and TGFβ-regulated Smad3. *Nat. Commun.* **7,** 11642 (2016).
3. Lang, M. *et al.* The soluble guanylate cyclase stimulator riociguat ameliorates pulmonary hypertension induced by hypoxia and SU5416 in rats. *PLoS One* **7,** (2012).
4. Tabeling, C. *et al.* CFTR and sphingolipids mediate hypoxic pulmonary vasoconstriction. *Proc. Natl. Acad. Sci. U. S. A.* **112,** E1614–23 (2015).

Supplementary figure legends:

Suppl. Fig. 1: Serial sections of human lungs from healthy donors or IPAH patients were immunohistochemically stained (in red) for SMAD3 (left) or smooth muscle actin (SMA; right). Nuclei were counterstained blue with Hematoxylin. Lower panels show enlarged areas as indicated in top panels.

Suppl. Fig. 2: HuPASMC (A, B) and huPAEC (C, D) were treated either with platelet-derived growth factor (PDGF; 10ng/mL and 100ng/mL) or interleukin-6 (IL-6; 10ng/mL or 100ng/mL) and probed for SMAD3 protein expression. Representative western blots are shown in A,C and quantitative data in B,D (n=7-8 each; **P*<0.05 vs. control, CTL).

Suppl. Fig. 3: Effect of 24h and 48h treatment with either 1µMol/L or 5µMol/L CCG1423 on activated caspase 3 expression as measured by flow cytometry in either huPASMC (A) or huPAEC (B). Staurosporine (0.1 µMol/L) served as positive control. Representative

histograms and quantitative data for the percentage of activated caspase 3 positive cells are shown (n=3 each; *P<0.05 vs. corresponding time control, CTL).

Suppl. Fig. 4: Effect of 24h and 48h treatment with either 1µMol/L or 5µMol/L CCG1423 on Poly (ADP-ribose) polymerase (PARP) cleavage in either huPASMC (A) or huPAEC (B). Staurosporine (0.1 µMol/L) served as positive control. Representative western blots for total PARP, cleaved PARP and GAPDH as loading control are shown as well as quantitative data for cleaved PARP normalized either to total PARP or GAPDH, respectively (n=4 each; *P<0.05 vs. corresponding time control, CTL).

Suppl. Fig. 5: Ki-67 expression is decreased in SMAD3 overexpressing huPASMCs following 72h stimulation with 5ng/ml TGF-β and 24h with 5% FCS. Ki-67 positivity was determined by flow cytometry in GFP positive cells overexpressing either GFP-linked control (CTL) plasmid or GFP-linked SMAD3 plasmid, treated with or without TGF-β and/or FCS (n=3 each; *P<0.05 vs CTL-CTLplasmid.

Suppl. Fig. 6: (A) Uncropped western blot shown in Figure 5C. (B) Alternative to Figure 3C PCNA western blot quantification summary. Data was normalized to siCTL